Supporting Information

A case study of Pd…Pd intramolecular interaction in benzothiazole based Palladacycle; Catalytic activity toward amides synthesis via isocyanide insertion pathway

Masood Loni, Yaser Balmohammadi, Reza Dadgar Yeganeh, Kaveh Imani, Behrouz Notash, Ayoob Bazgir

Department of Chemistry, Shahid Beheshti University G.C., Tehran 1983963113, Iran

a_bazgir@sbu.ac.ir

Table of Contents

Crystal data and structure refinement for BTP……...…..2
Computational studies of Pd…Pd interaction in BTP……..…2-6
EDX …….…6
P-XRD…… 6
FT-IR……....7
TGA…….....8
BET Curve……8
BET results…….....9
SEM……..9
TEM……... ..9
Proposed mechanism of MIIr catalyzed by BTP@SBA.....11-17
References……..17
Copy of NMR of amides 6……18-31

Crystal data and structure refinement for BTP

Identification code	khc1445b
Empirical formula	C31 H26 N2 O7 Pd2 S2
Formula weight	815.46
Temperature	298(2) K
Wavelength	0.71073 A
Crystal system, space group	Orthorhombic, P 21 21 21
Unit cell dimensions	a = 7.9107(16) A alpha = 90 deg.
	b = 12.229(2) A beta = 90 deg.
	c = 30.953(6) A gamma = 90 deg.
Volume	2994.4(10) A^3
Z, Calculated density	4, 1.809 Mg/m^3
Absorption coefficient	1.392 mm^-1
F(000)	1624
Crystal size	0.20 x 0.15 x 0.15 mm
Theta range for data collection	2.58 to 24.99 deg.
Limiting indices	-8<=h<=9, -12<=k<=14, -32<=l<=36
Reflections collected / unique	9420 / 5207 [R(int) = 0.0967]
Completeness to theta = 24.99	99.9 %
Absorption correction	Numerical
Max. and min. transmission	0.8183 and 0.7681
Refinement method	Full-matrix least-squares on F^2
Data / restraints / parameters	5207 / 0 / 403
Goodness-of-fit on F^2	0.960
Final R indices [I>2 sigma(I)]	R1 = 0.0595, wR2 = 0.1257
R indices (all data)	R1 = 0.0897, wR2 = 0.1473
Absolute structure parameter	0.05(7)
Largest diff. peak and hole	0.915 and -0.576 e.A^-3

Computational studies of Pd…Pd interaction in BTP

Computational details

DFT calculation for constructing theoretical wave function and NBO analysis have been carried out using the Gaussian 09 suite of programs[1]. The selected fragment involved with Pd…Pd interaction was cut out directly from the CIF file and after that it is optimized using B3LYP[2] functional and LANL2DZ[3] basis set. The QTAIM analysis of theoretical charge density is performed using the AIMALL program[4]. The NCI-RDG analysis is performed using Multiwfn program[5]. The gradient isosurface of NCI-RDG is visualized by using the VMD 1.9.2 software[6]. HOMO and LUMO molecular orbitals are depicted using GaussView 5.0software [1].

Comparison of selected geometric parameters of experimental structure with optimized one

Geometric Parameter	Experimental structure	Optimized Structure
Distances(Å)		
Pd1-Pd2	2.862	3.195
Pd2-C30	1.936	1.996
Pd2-O2	2.033	2.077
Pd2-O4	2.130	2.172
Pd2-N2	2.048	2.079
Pd1-O1	2.171	2.173
Pd1-O3	2.053	2.076
Pd1-C9	1.950	1.996
Pd1-N1	2.037	2.079
Angles(°)		
N2-Pd2-C30	81.95	81.06
N2-Pd2-O4	97.60	98.06
C30-Pd2-O2	91.82	92.60
O2-Pd2-O4	88.67	88.23
O1-Pd1-O3	86.02	88.23
O1-Pd1-N1	98.94	98.09
C9-Pd1-O3	92.31	92.62
N1-Pd1-C9	82.70	81.08

Topological and energetic properties at the Bond Critical Points between Palladium atoms involved in Pd…Pd interaction

Basis set	FUNCTIONAL	ρBCP	∇^2ρBCP	G(BCP)	V(BCP)	H(BCP)	|V(BCP)|/G(BCP)
LANL2DZ	B3LYP	0.0171	0.0477	0.0115	-0.0111	0.0004	0.965

Hirshfield analysis of Pd1…Pd2 axis

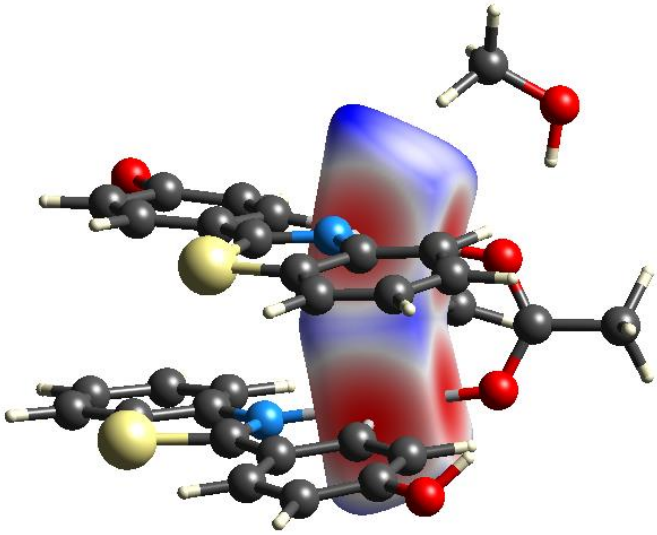

Figure 1. Electrostatic potential of Pd1…Pd2 axis analyze by Hirshfield diagram. The High electron density depicted as Red and low electron density as Blue

Contour map of Pd…Pd interaction

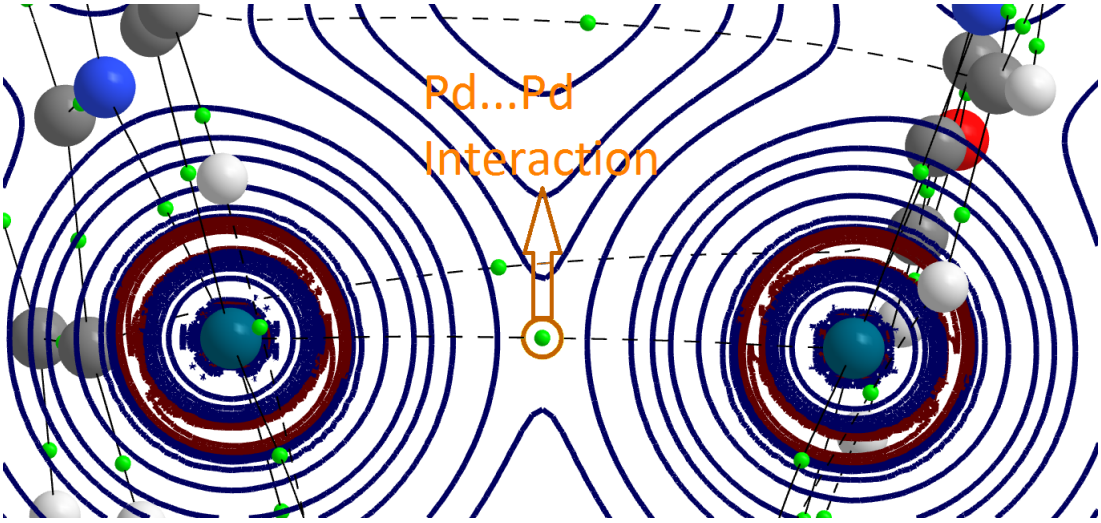

Figure 2. Scheme of contour map of Laplacian of electron density in B3LYP/LANL2DZ computational level. The BCP and positive value of Laplacian for Pd…Pd interaction are represented.

HOMO and LUMO Molecular orbitals

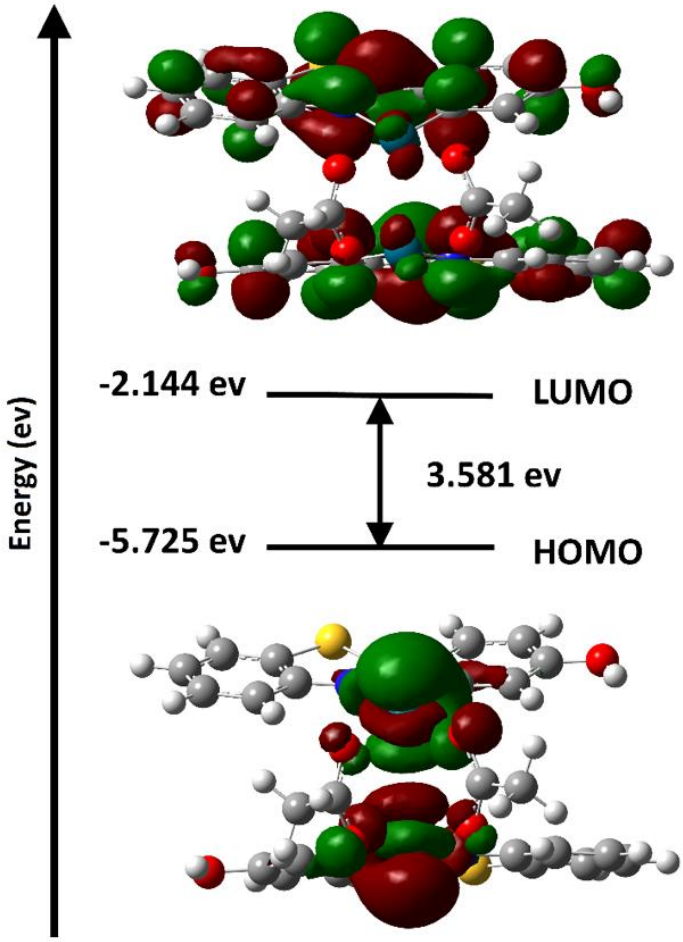

Figure 3. The HOMO and LUMO orbitals of the system and the energy gap between them

Reduced density gradient analysis

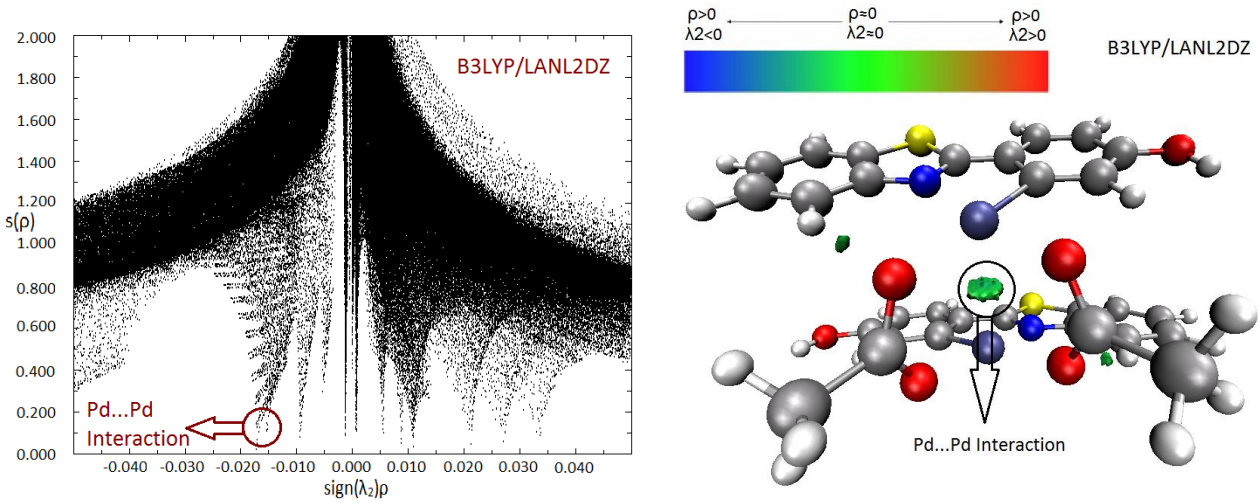

Figure 4. The plots of RDG, s(ρ), versus sign(λ2)ρ (Left) and colored s(ρ)-isosurface in B3LYP/LANL2DZ computational method (Right).

Bond Order By NBO analysis

The bond orderof the Pd···Pdinteraction was calculated by twoNBO criteria; Wiberg bond indices and NAO (natural atomic orbital) bond order. The positivevalue of the bond order determined by NAO indicates the existence of a net bonding interaction between Pd···Pd.

Calculated Bond Orders of Pd•••Pd Interaction

NBO criteria	Bond Order of Pd…Pd interaction
Wibergbond indices	0.0912
NAO bond order	0.1814

EDX

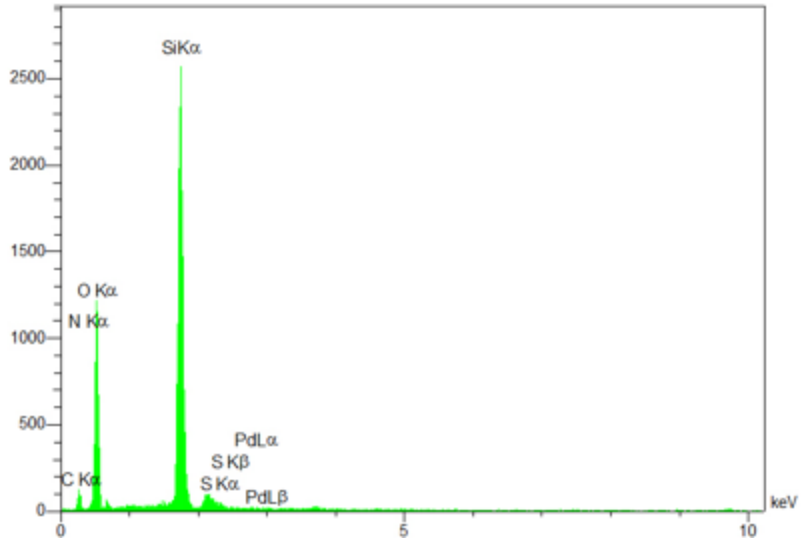

Figure 5. The EDX elemental analysis of BTP@SBA

P-XRD

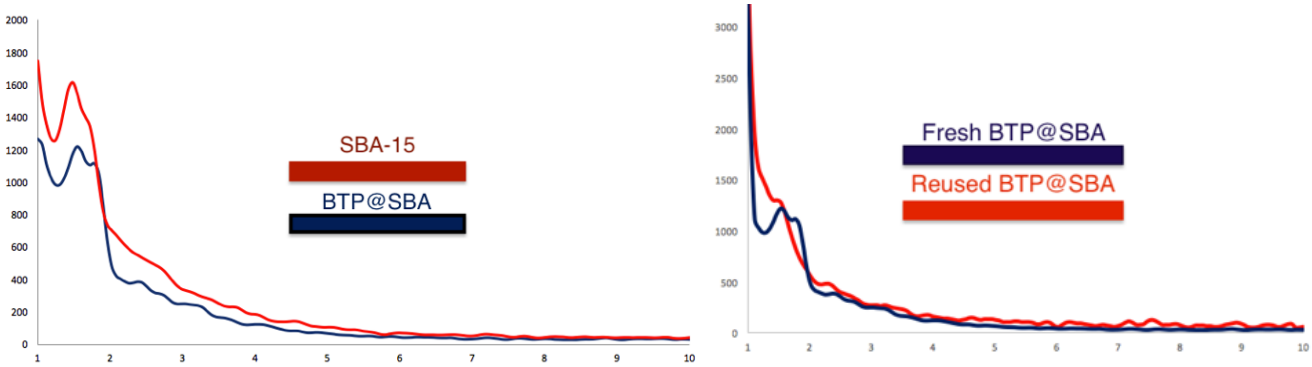

(A) **(B)**

Figure 6. The low angle P-XRD of BTP@SBA (A). Reused BTP@SBA after five catalytic cycle (B).

FT-IR

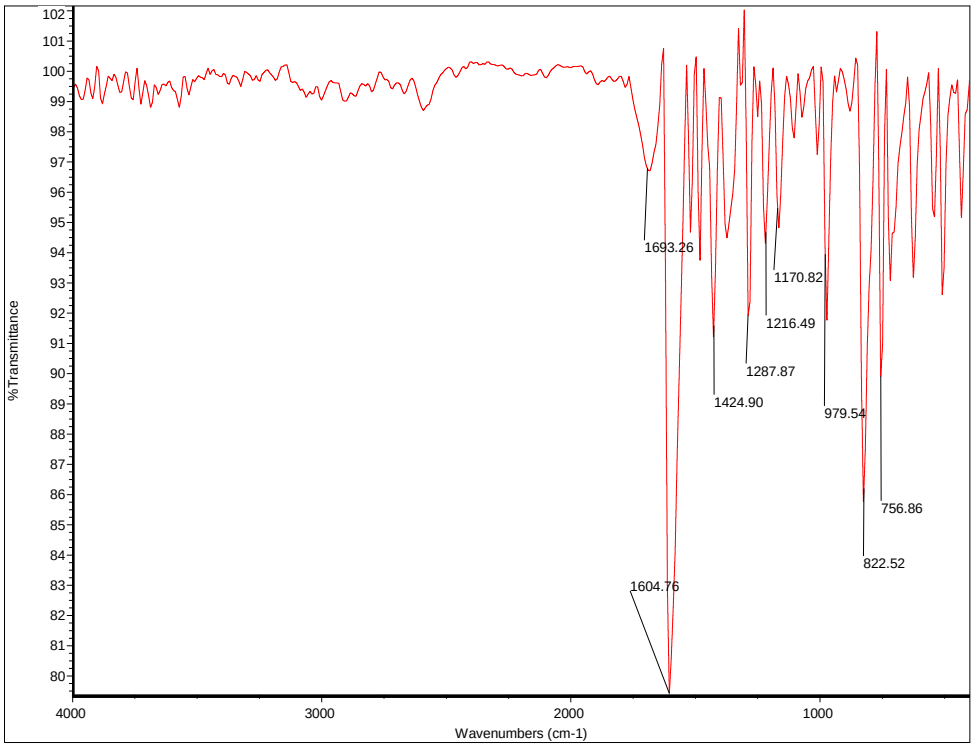

Figure 7. The schematic FT-IR spectrum of BTP

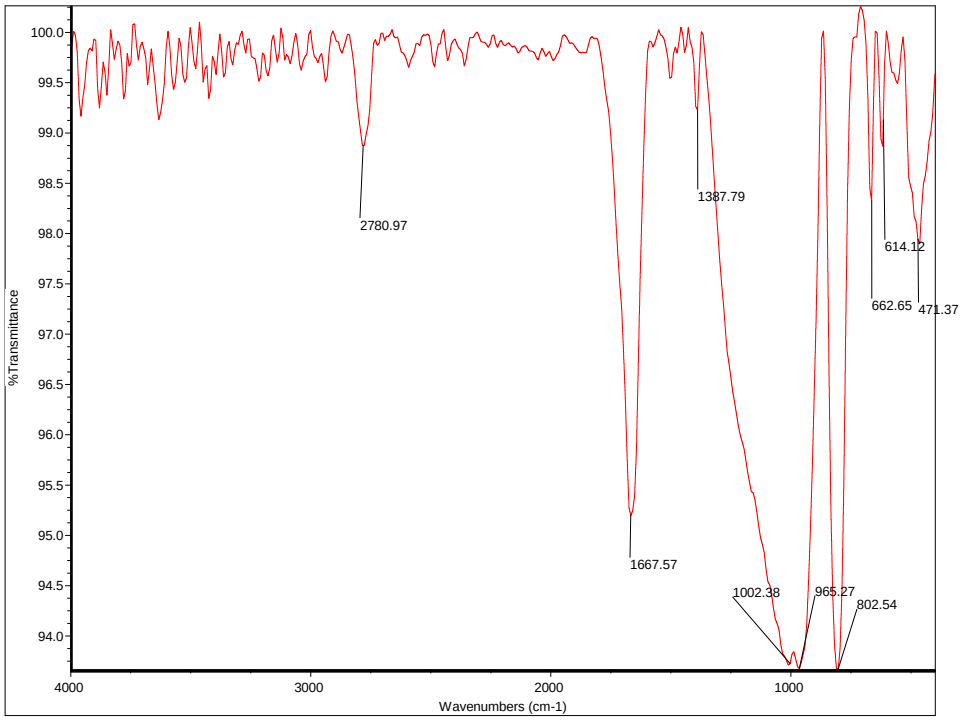

Figure 8. The schematic FT-IR spectrum of BTP@SBA-15

Details of FT-IR spectra

Entry	BTP	BTP@SBA
1	703 (C-S)	802 (Si-O)[a]
2	1604 (Aromatic C-H)	1002 (Si-O)[b]
3	1693 (C=O)	1667 (C=O)
4	2820 (Acetate C-H)	2780 (Acetate C-H)

a: Bending
b: Stretching

TGA

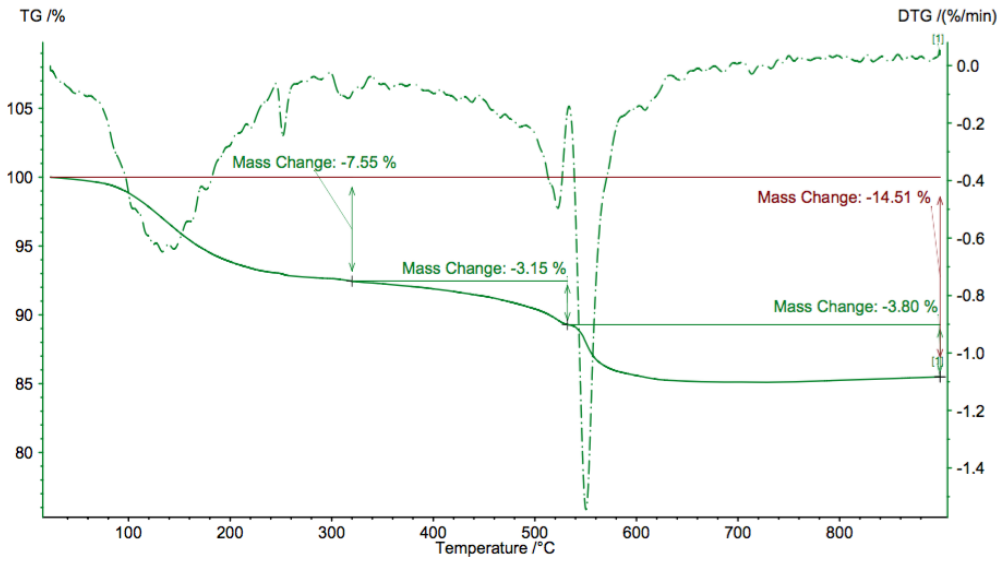

Figure 9. The TGA of BTP@SBA up to 900 °C..

BET curve

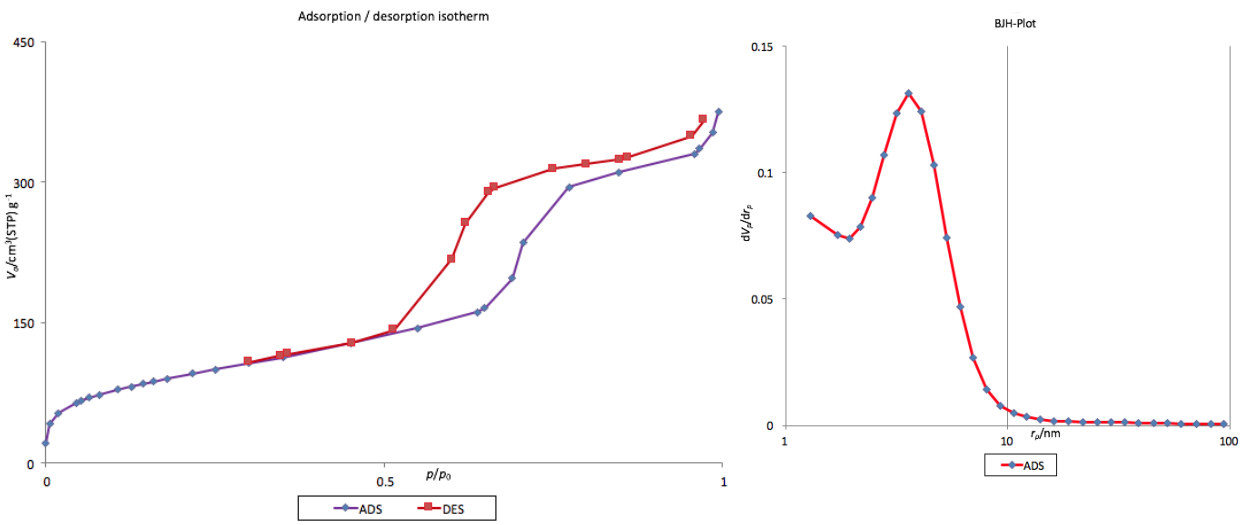

Figure 10. The Bet curve of BTP@SBA (A) and BJH distribution curve of BTP@SBA (B)

BET results

The N_2(g) adsorption analysis of BTP@SBA and fresh SBA-15.

	BET plot of **(4)**	Fresh SBA-15	Unit
V_m	75.661	103.743	[cm^3(STP) g^{-1}]
$a_{s,BET}$	329.31	726.6	[m^2 g^{-1}]
Total pore volume(p/p_0=0.990)	0.5629	0.9842	[cm^3 g^{-1}]
Mean pore diameter	6.8368	9.2687	[nm]

SEM

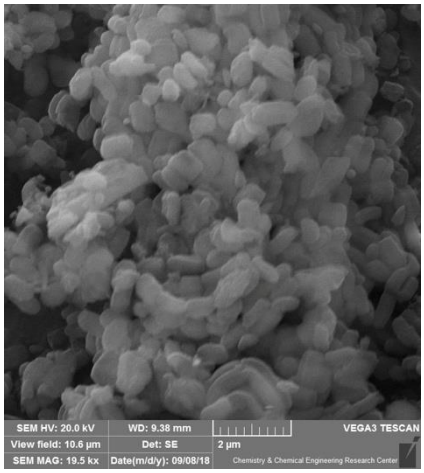

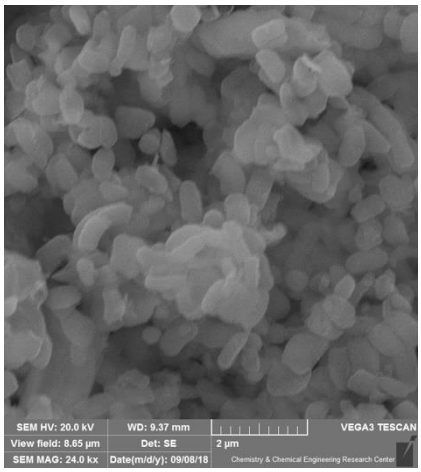

(A) (B)

Figure 11. The SEM image of BTP@SBA (A) and Reused BTP@SBA after 5 catalytic cycle (B)

TEM

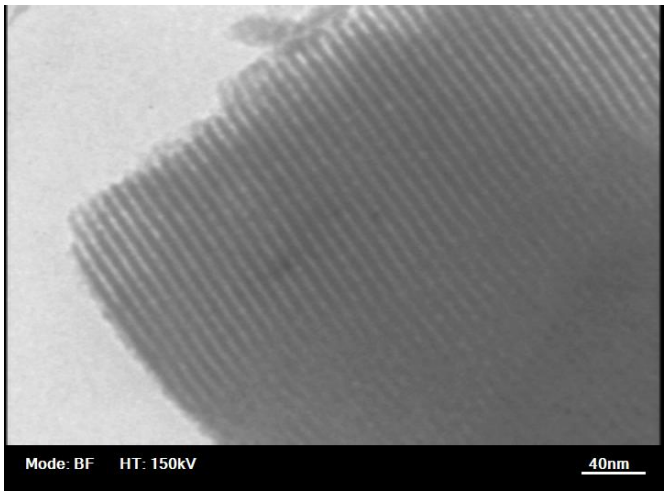

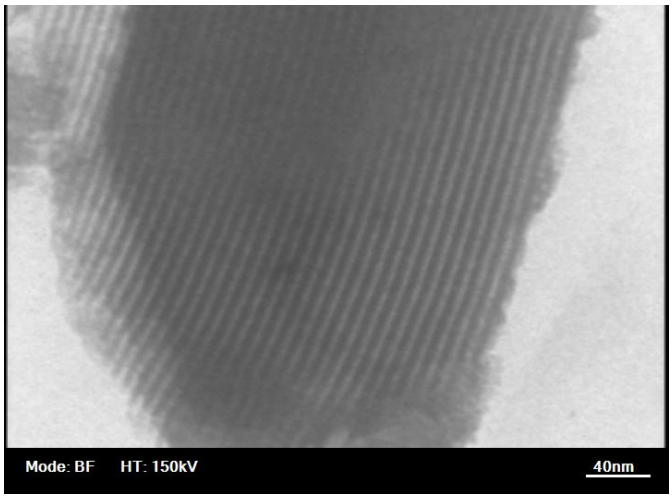

(A) (B)

Figure 12. The TEM of BTP@SBA along to pore axis of BTP@SBA (B) and reused BTP@SBA after 5 catalytic cycle (B)

Proposed mechanism of MIIr catalyzed by BTP@SBA

The proposed mechanism of MIIr catalyzed by BTP@SBAstart by exchange of OAc^- by DMSO as solvent, that is common in palladaium coordinated acetate moieties[7]. It is noticeable, all of the reports of MIIr mostly work in DMSO/H_2O solvent conditions. The oxidative addition of Ph-I to Pd(II) center afford Pd(IV) as octahedral six coordinated complex (c). Subsequently, the isocyanide coordinate to Pd(IV) and DMSO get out from the coordination sphere (d). By the migratory isocyanide insertion to Pd-Ph and reinstallation of DMSO the coordinated PhC=NR moiety obtained. The DFT calculation MIIr catalyzed by $PdCl_2$ elucidate the OH^-substitution by iodide to form Pd-OH intermediate[8]. The iminol or imidic acid formattained after reductive elimination of OH^- and PhC=NR group. The resulting MIIr was taken by the tautomerization of imidic acid to amide. Notably, the paladacycle (b) was proposed as actual catalyst of MIIr.

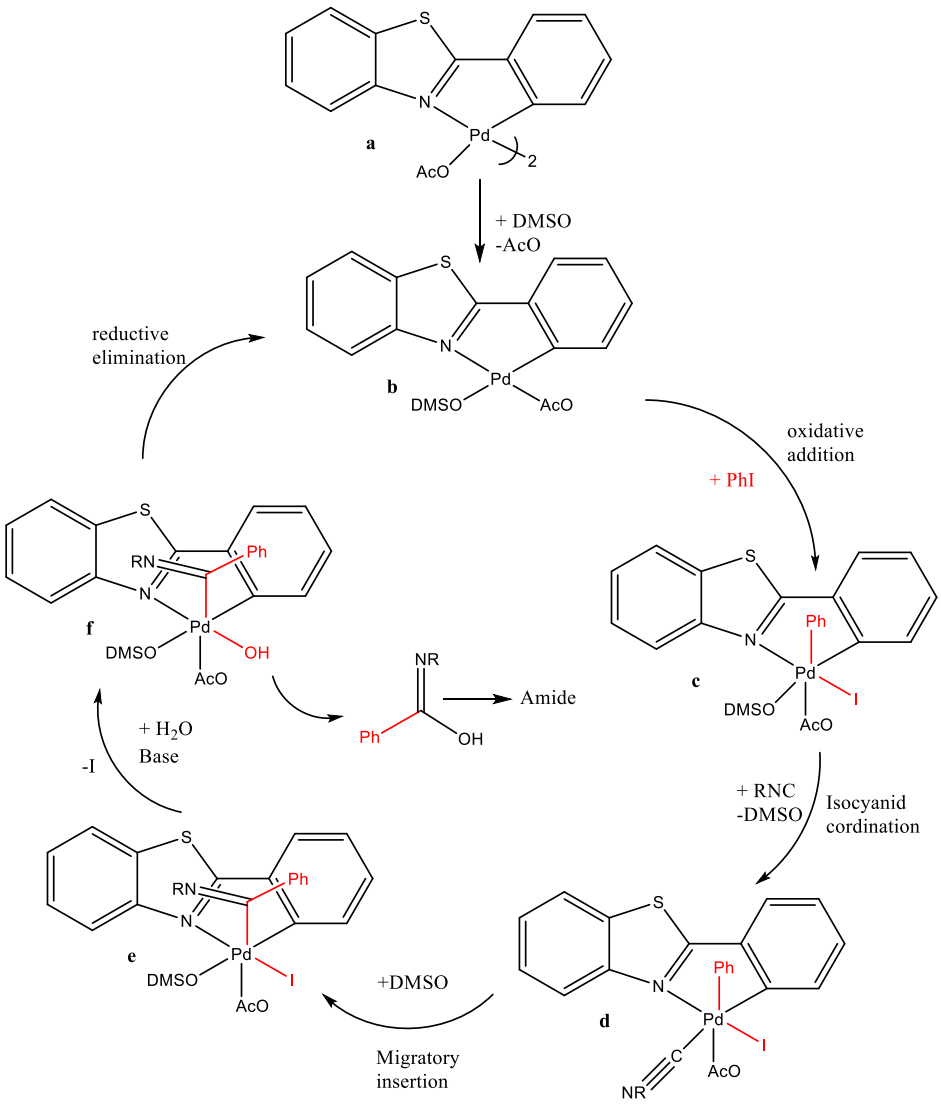

Figure 13. Proposed mechanism of BTP@SBA catalyze MIIr via Pd(+2)/Pd(+4) catalytic cycle

Experimental

Materials and measurement

All chemicals were purchased from Merck or Aldrich and were used without additional distillation. FT-IR spectra were taken with a Bomem FT-IR MB spectrometer. The NMR spectra were recorded on a BRUKER DRX-300 AVANCE spectrometer. Powder X-RAY Diffraction data were collected on a STOE STADI P with scintillation detector, secondary monochromator and Cu-Ka1 radiation (λ =1. 5406 Å). EDS characterizations of BTP@SBA were performed using an electron microscopy Philips XL-30 ESEM. Transmission Electron Microscopy characterization of BTP@SBA was performed using a transmission microscope Philips CM-30 with an accelerating voltage of 150 kV. The concentration of Pd was estimated using Shimadzu AA-680 flame atomic absorption spectrophotometer. The sorption analysis was recorded by micromeritics Auto-chem II 2920. Furthermore, The TGA was accomplished by Perkin Elmer TGA/DSC. Lastly, the CHNS content was estimated by Perkin Elmer 2400 series.

The X-ray diffraction measurements were made with a STOE IPDS-II diffractometer with graphite-monochromated MoKa radiation. Cell constants and an orientation matrix for data collection were obtained by least-squares refinement of diffraction data from 6743 and 3408 unique reflections for BTP. Data were collected at a temperature of 298(2) K to a maximum 2q value of 51.988 and in a series of w scans in 18 oscillations and integrated using the Stoe X-AREA software package. The data were corrected for Lorentz and Polarizing effects. The structures were solved by direct methods and refined on F2 by full-matrix least-squares procedure. All hydrogen atoms were added at ideal positions and constrained to ride on their parent atoms, with Uiso(H)= 1.2Ueq. All refinements were performed by using the X-STEP32 crystallographic software package. Complete crystallographic data for BTP has been deposited with the Cambridge Crystallographic Data Centre as supplementary publication No. CCDC 1968870. These data can be obtained free of charge from The Cambridge Crystallographic Data Centre via www.ccdc.cam.ac.uk/data_request/cif.

Synthesis of 4-Hydroxy 2-Phenyl Benzothiazole (3)

The 2-aminothiophenol (1mmol) and 4-hydroxybenzaldehyde (1mmol) stirred in MeOH at room temperature to afford yellow imine sediment. Subsequently, NH_2SO_3H (10 mol%) was added to the reaction mixture. After 4h, light yellow sediment achieved and recrystallized in MeOH/H_2O to afford pure product. Melting point: 227-230 ºC.^{1}H NMR (300 MHz, DMSO): 10.22 (1H, s, OH), 8.06 (1H, d, $^3J_{HH}$ = 9.0 Hz, H–Ar), 7.95 (3H, m, H–Ar), 7.48 (1H, t, $^3J_{HH}$ = 9.0 Hz, H–Ar), 7.38 (1H, t, $^3J_{HH}$ = 9.0 Hz, H–Ar), 6.93 (2H, d, $^3J_{HH}$ = 9.0 Hz, H–Ar). Anal. Calcd for $C_{13}H_9NOS$: C, 68.70; H, 3.99; N, 6.16. Found: C, 66.27; H, 4.15; N, 6.05.

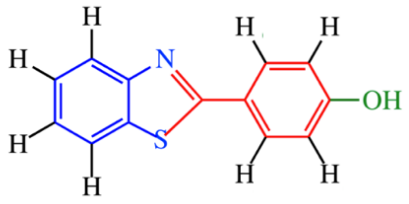

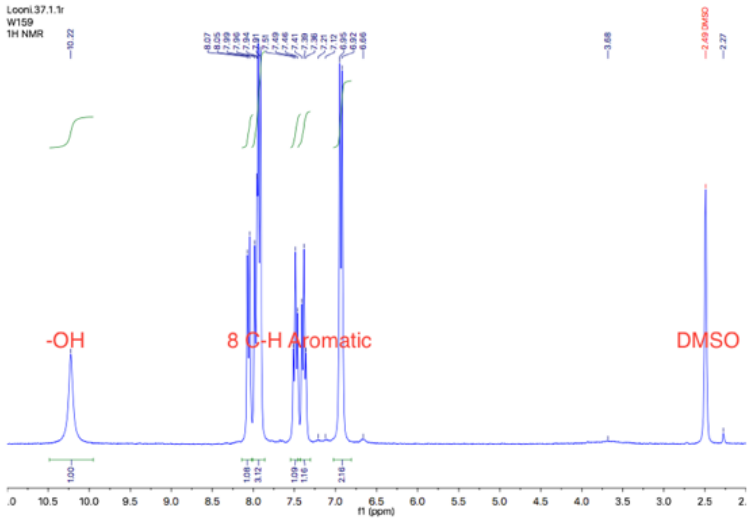

Synthesis of 4-hydroxy 2-phenyl benzothiazole palladacycle (BTP)

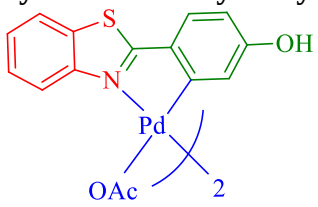

The dimeric acetate palladacycle **(BTP)** was obtained by the reaction of **(3)** (1mmol) and $Pd(OAc)_2$ (1mmol) in HOAc under reflux conditions and inert atmosphere for 2h. Afterward, the excess amount of N-hexane was added to the reaction mixture and the sediment gained by simple filtration as greyish-green color.^{1}H NMR (300 MHz, DMSO). 9.39 (1H, s, OH), 7.61 (1H, d, $^3J_{HH}$ = 9.0 Hz, H–Ar), 7.50 (1H, d,$^3J_{HH}$ = 9.0 Hz, H–Ar), 7.19 (2H, m, H–Ar), 6.71 (1H, d, $^3J_{HH}$ = 9.0 Hz, H–Ar), 5.81 (1H, s, H–Ar), 5.70 (1H, d, $^3J_{HH}$ = 9.0 Hz, H–Ar), 2.18 (3H, s, Me).MS (EI, 70 eV) m/z: 391 (M^+/2). Anal. Calcd for $C_{30}H_{22}N_2O_6Pd_2S_2$: C, 45.99; H, 2.83; N, 3.58. Found: C, 45.68; H, 2.71; N, 3.41.

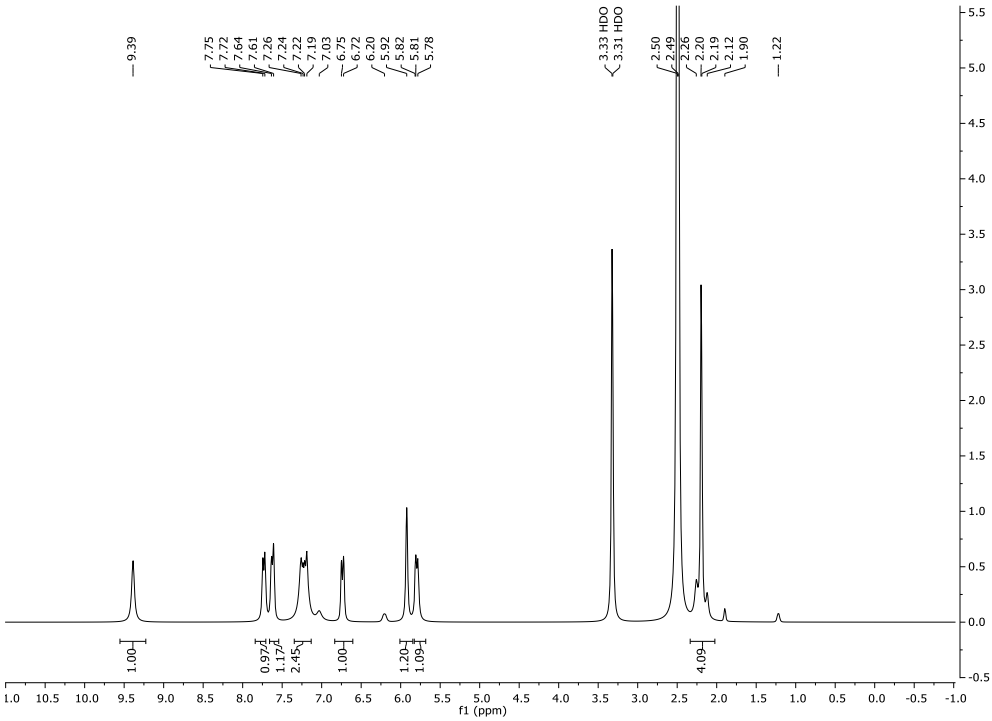

Mass Spectrum of BTP

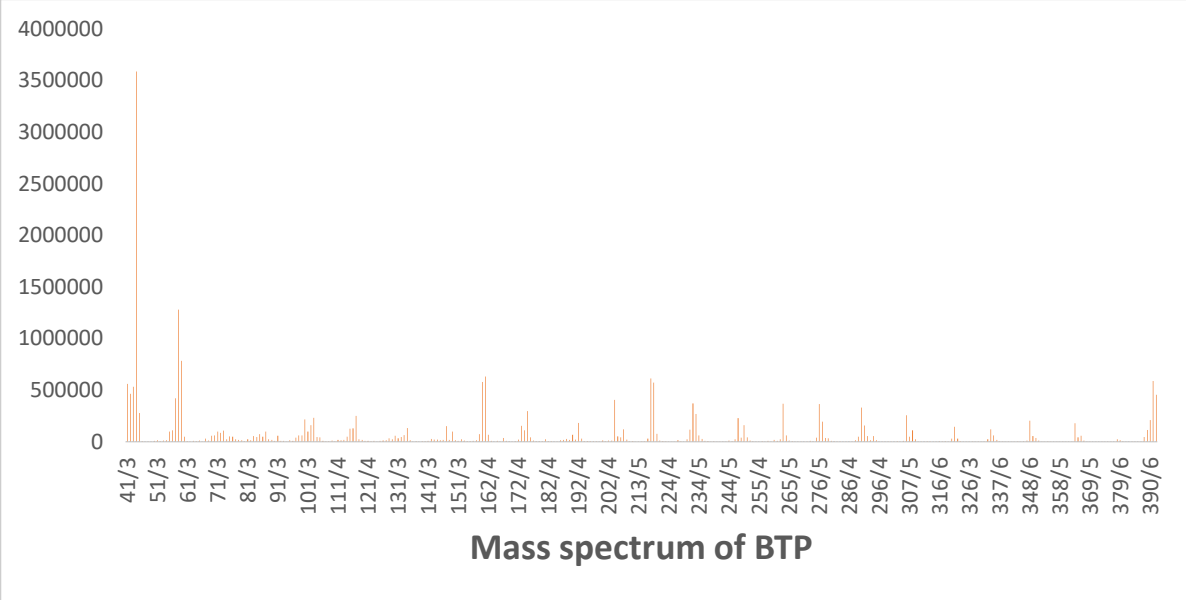

Figure 14. Mass spectrum of BTP

Synthesis of chlorinated SBA-15

The fresh SBA-15 was kept overnight under 120 ^{o}C to evaporate adsorbed water. The SBA-Cl was obtained by chlorination of dried SBA-15 nanoparticles. SBA-15 (3 g) was refluxed in 60 mlit $SOCl_2$ in a round bottomed flask fortified with a drying tube, condenser and inert atmosphere for 24h. The excess amount of thionyl chloride was distilled off and the resulting solid product was flame-dried as light-greyish color and stored in a sealed vessel under N_2(g).

Synthesis of BTP directly bonded to SBA-15 (BTP@SBA)

The BTP (0.5 mmol, 0.39 gr) was dissolved in 40 mL dried DMF. The soluble of BTP was added drop wise to the round bottom flask containing dried chlorinated SBA-15 under N_2(g). The reaction accompanied by emission of gaseous HCl. The reaction was stirred for 24h at room temperature. Then, the 60 ml of MeOH was added to the reaction. Afterward, the BTP@SBA was separated by centrifuge and washed several times with MeOH and H_2O in order to neutralize the PH.

General procedure for the migratory isocyanide insertion reaction (MIIr)

A mixture of arylhalides (1mmol), isocyanides (1.2 mmol) and Cs_2CO_3 (1mmol) in presence of 0.5 mol% of BTP@SBA in DMSO/H_2O (2 mL, 1:1) was stirred at 100 ^{o}C for 24h. After completion of the reaction (TLC), the reaction mixture was cooled to room temperature. Then, MeOH (5 mL) was added to the reaction mixture and the solid BTP@SBA was separated by filtration. The filtrate was

evaporated under vacuum and the product was purified by Column chromatography (EtOAc/n-Hexane (3/7).

All of the synthesized amide are known compounds.[9-13]

N-(tert-butyl)benzamide (6a).

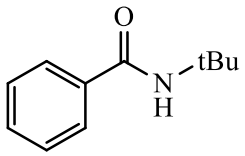

Cream powder; m.p. 131-133 ˚C. IR (KBr) (νmax /cm^{-1}): 3327, 3064, 2975, 1642, 1449. ^{1}H NMR (300 MHz, $CDCl_3$) δ 1.51 (s, 9H), 6.10 (brs, 1H), 7.30 -7.51 (m, 3H), 7.71-7.83 (m, 2H). ^{13}C NMR (75 MHz, $CDCl_3$) δ 28.9, 51.6, 126.8, 128.4, 131.0, 135.9, 167.0.

N-cyclohexylbenzamide (6b).

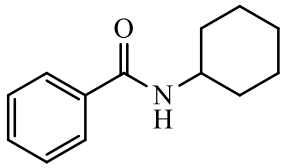

White powder; m.p. 151-153 ˚C. IR (KBr) (νmax /cm^{-1}): 3301, 3215, 2938, 1659. ^{1}H NMR (300 MHz, $CDCl_3$) δ 1.21-1.52 (m, 6H), 1.71-1.83 (m, 2H), 2.01-2.12 (m, 2H), 4.00-4.10 (m, 1H), 6.10 (brs, 1H), 7.31-7.52 (m, 3H), 7.81-7.83 (m, 2H). ^{13}C NMR (75 MHz, $CDCl_3$) δ 24.9, 25.6, 33.3, 48.7, 126.8, 128.5, 131.2, 135.1, 166.6.

N-(2,4,4-trimethylpentan-2-yl)benzamide (6c).

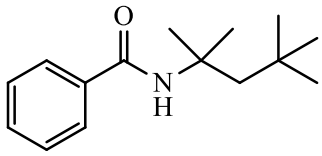

White powder; m.p. 70-72 ˚C. IR (KBr) (νmax /cm^{-1}): 3311, 2920, 1650, 1456. ^{1}H NMR (300 MHz, $CDCl_3$) δ 1.01 (s, 9H), 1.50 (s, 6H), 1.83 (s, 2H), 5.96 (brs, 1H), 7.36-7.48 (m, 3H), 7.67-7.68 (m, 2H). ^{13}C NMR (75 MHz, $CDCl_3$) δ 29.7, 31.5, 31.7, 51.8, 55.1, 126.1, 128.4, 130.5, 135.7, 166.3.

N-(2,6-dimethylphenyl)benzamide (6d).

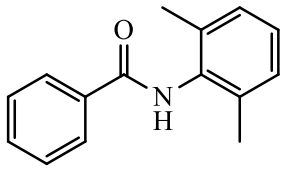

Yellow powder; m.p. 158-160 ˚C. IR (KBr) (νmax /cm^{-1}): 3285, 1654, 1534, 1465. ^{1}H NMR (300 MHz, $CDCl_3$) δ 2.14 (s, 9H), 4.64 (brs, 1H), 7.13 (s, 3H), 7.43 (d, J = 9.1 Hz, 2H), 7.95 (d, J = 9.1 Hz, 2H). ^{13}C NMR (75 MHz, $CDCl_3$) δ 18.5, 127.2, 127.4, 128.3, 131.8, 133.8, 134.3, 135.5, 165.8.

N-cyclohexyl-4-methylbenzamide (6e).

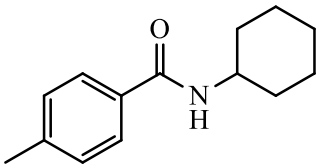

Cream powder; m.p. 160-162 ˚C. IR (KBr) (νmax /cm^{-1}): 3323, 2918, 1643, 1556. ^{1}H NMR (300 MHz, $CDCl_3$) δ 1.31-1.45 (m, 6H), 1.61-1.66 (m, 2H), 1.72-2.01 (m, 2H), 2.41 (s, 3H), 4.01 (m, 1H), 6.21 (brs, 1H), 7.21 (d, *J* = 7.7 Hz, 2H), 7.70 (d, *J* = 7.7 Hz, 2H). ^{13}C NMR (75 MHz, $CDCl_3$) δ 21.4, 25.0, 25.6, 33.2, 48.6, 126.9, 129.1, 132.2, 141.5, 166.6.

N-cyclohexyl-2-methylbenzamide (6f).

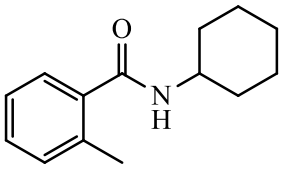

White powder; m.p. 157-159 ˚C. IR (KBr) (νmax /cm^{-1}): 3334, 2932, 2843, 1662, 1565. ^{1}H NMR (300 MHz, $CDCl_3$) δ 1.22-1.43 (m, 6H), 1.71-1.83 (m, 2H), 1.86– 2.10 (m, 2H), 2.22 (s, 3H), 4.02 (m, 1H), 6.53 (brs, 1H), 7.21-7.43 (m, 4H). ^{13}C NMR (75 MHz, $CDCl_3$) δ 19.7, 24.9, 25.6, 48.5, 125.7, 126.6, 129.6, 130.9, 135.7, 137.0, 169.3.

N-(tert-butyl)-4-methoxybenzamide (6g).

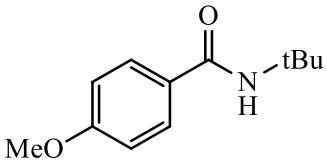

White powder; m.p. 116-118 ˚C. IR (KBr) (νmax /cm^{-1}): 3348, 3074, 2856, 1665, 1553, 1450. ^{1}H NMR (300 MHz, $CDCl_3$) δ 1.51 (s, 9H), 3.83 (s, 3H), 6.01 (brs, 1H), 6.91-6.93 (m, 2H), 7.71-7.73 (m, 2H). ^{13}C NMR (75 MHz, $CDCl_3$) δ 28.9, 51.4, 55.4, 113.6, 128.2, 128.5, 161.8, 166.5.

N-cyclohexyl-4-methoxybenzamide (6h).

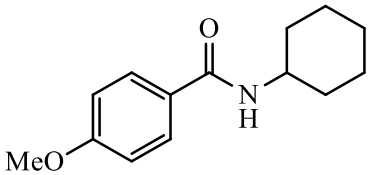

Cream powder; m.p. 158-160-228 ˚C. IR (KBr) (νmax /cm^{-1}): 3392, 2850, 1667. ^{1}H NMR (300 MHz, $CDCl_3$) δ 1.24-1.53 (m, 6H), 1.63-1.77 (m, 2H), 1.81– 2.02 (m, 2H), 3.91 (s, 3H), 4.03 (m, 1H), 6.22 (brs, 1H), 6.92 (d, *J* = 7.9 Hz, 2H), 7.73 (d, *J* = 7.9 Hz, 2H). ^{13}C NMR (75 MHz, $CDCl_3$) δ 25.0, 25.6, 33.3, 48.6, 55.4, 113.6, 127.4, 128.7, 161.9, 166.2.

N-(tert-butyl)-4-nitrobenzamide (6i).

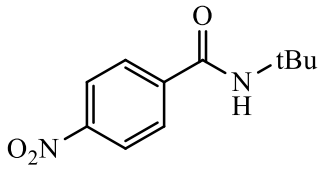

Yellow powder; m.p. 160-162 ˚C. IR (KBr) (νmax /cm^{-1}): 3321, 3062, 2970, 1645. ^{1}H NMR (300 MHz, $CDCl_3$) δ 1.53 (s, 9H), 6.11 (brs, 1H), 7.93 (d, *J* = 8.1 Hz, 2H), 8.21 (d, *J* = 8.1 Hz, 2H). ^{13}C NMR (75 MHz, $CDCl_3$) δ 28.7, 52.3, 123.7, 128.0, 141.6, 149.3, 164.9.

4-acetyl-N-(tert-butyl)benzamide (6j).

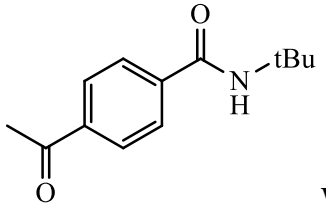

White powder; m.p. 140-142 ˚C. IR (KBr) (νmax /cm^{-1}): 3305, 2970, 1678, 1535. ^{1}H NMR (300 MHz, $CDCl_3$) δ 1.50 (s, 9H), 2.61 (s, 3H), 6.12 (brs, 1H), 7.82 (d, *J* = 6.8 Hz, 2H), 8.02 (d, *J* = 6.8 Hz, 2H). ^{13}C NMR (75 MHz, $CDCl_3$) 26.8, 28.8, 52.0, 127.1, 128.4, 138.8, 139.8, 165.9, 197.5.

4-acetyl-N-cyclohexylbenzamide (6k).

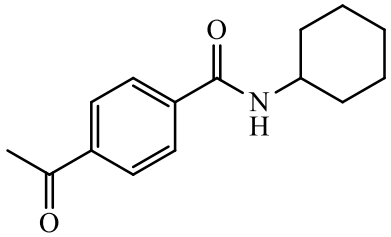

White powder; m.p. 196-198 ˚C. IR (KBr) (νmax /cm^{-1}): 3318, 2911, 1689, 1637, 1478. ^{1}H NMR (300 MHz, $CDCl_3$) δ 1.31-1.71 (m, 6H), 1.74-1.91 (m, 2H), 1.97– 2.21 (m, 2H), 2.63 (s, 3H), 4.02 (m, 1H), 6.20 (brs, 1H), 7.83 (d, *J* = 7.6 Hz, 2H), 8.04 (d, *J* = 7.6 Hz, 2H). ^{13}C NMR (75 MHz, $CDCl_3$) δ 24.9, 25.5, 26.8, 33.1, 49.0, 127.2, 128.4, 138.9, 139.0, 165.7, 197.5.

N-(2,6-dimethylphenyl)-4-methylbenzamide (6l).

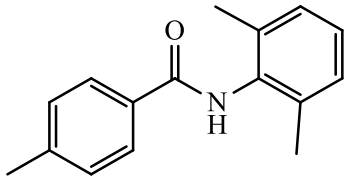

White powder; m.p. 163-165 ˚C. IR (KBr) (νmax /cm^{-1}): 3318, 2911, 1689, 1637, 1478. ^{1}H NMR (300 MHz, $CDCl_3$) δ 2.43 (m, 6H), 2.62 (s, 3H), 7.15 (s, 3H), 7.16-7.19 (m, 2H), 7.20 (s, 1H), 7.86 (d, *J* = 6.5 Hz, 2H). ^{13}C NMR (75 MHz, $CDCl_3$) δ 17.8, 21.4, 127.1, 127.4, 128.3, 129.0, 131.8, 133.8, 134.5, 135.5, 166.0.

N-(tert-butyl)picolinamide (6m).

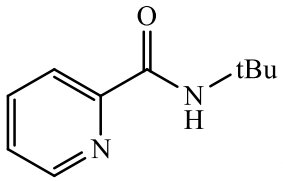

Yellow powder; m.p. 35-37 ˚C. IR (KBr) (νmax /cm^{-1}): 3367, 2961, 2920, 1685. ^{1}H NMR (300 MHz, $CDCl_3$) δ 1.67 (s, 9H), 7.39 (t, *J* = 6.6 Hz, 1H), 7.79-7.84 (m, 1H), 7.96 (brs, 1H), 8.18 (d, *J* = 8.6 Hz, 1H), 8.53 (d, *J* = 4.5 Hz, 1H). ^{13}C NMR (75 MHz, $CDCl_3$) δ 28.9, 51.7, 123.4, 125.6, 138.9, 148.7, 153.4, 164.3.

N-cyclohexylpicolinamide (6n).

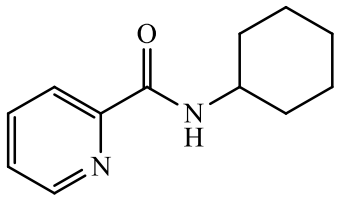

Cream powder; m.p. 55-57 ˚C. IR (KBr) (νmax /cm^{-1} 3371, 2931, 2851, 1660. ^{1}H NMR (300 MHz, $CDCl_3$) δ δ 1.31-1.67 (m, 6H), 1.71-1.85 (m, 2H), 1.87– 2.09 (m, 2H), 4.05 (m, 1H), 6.20 (brs, 1H), 7.41 (d, *J* = 7.2 Hz, 1H), 7.82-7.84 (m, 1H), 8.10 (brs, 1H), 8.22 (d, *J* = 7.6 Hz, 1H), 8.51 (d, *J* = 6.2 Hz, 1H). ^{13}C NMR (75 MHz, $CDCl_3$) δ 24.9, 25.6, 33.1, 48.1, 122.2, 126.0, 137.3, 147.9, 150.2, 163.2.

Reference

1. *M. J. Frisch, G. Trucks, H. Schlegel, G. Scuseria, M. Robb, J. Cheeseman, G. Scalmani, V. Barone, B. Mennucci and G. Petersson, Inc.: Wallingford, CT, 2009.*
2. *A. D. Becke, The Journal of Chemical Physics, 1993, 98, 5648-5652.*
3. *P. J. Hay and W. R. Wadt, The Journal of chemical physics, 1985, 82, 270-283.*
4. *T. Keith, Journal, 2010.*
5. *T. Lu and F. Chen, Journal of computational chemistry, 2012, 33, 580-592.*
6. *W. Humphrey, A. Dalke and K. Schulten, Journal of molecular graphics, 1996, 14, 33-38.*
7. *T. Diao, P. White, I. Guzei and S. S. Stahl, Inorganic Chemistry, 2012, 51, 11898-11909.*
8. *Y. Liang, Y. Ren, J. Jia and H.-S. Wu, Journal of molecular modeling, 2016, 22, 53.*
9. *H. Jiang, B. Liu, Y. Li, A. Wang and H. Huang, Organic Letters, 2011, 13, 1028-1031.*
10. *I. Yavari, M. Ghazanfarpour-Darjani and M. J. Bayat, Tetrahedron letters, 2014, 55, 4981-4982.*

11. Y. Jo, J. Ju, J. Choe, K.H. Song, S. Lee, S. J. Org. Chem. 2009, 74, 6358.

12. G. Bechara, W. S. Bechara, A. B. Charette, J. Am. Chem. Soc. 2010, 132, 12817.

13. M. Malacarne, S. Protti, M. Fagnoni, Advanced Synthesis and Catalysis, 2017, 359, 3826.

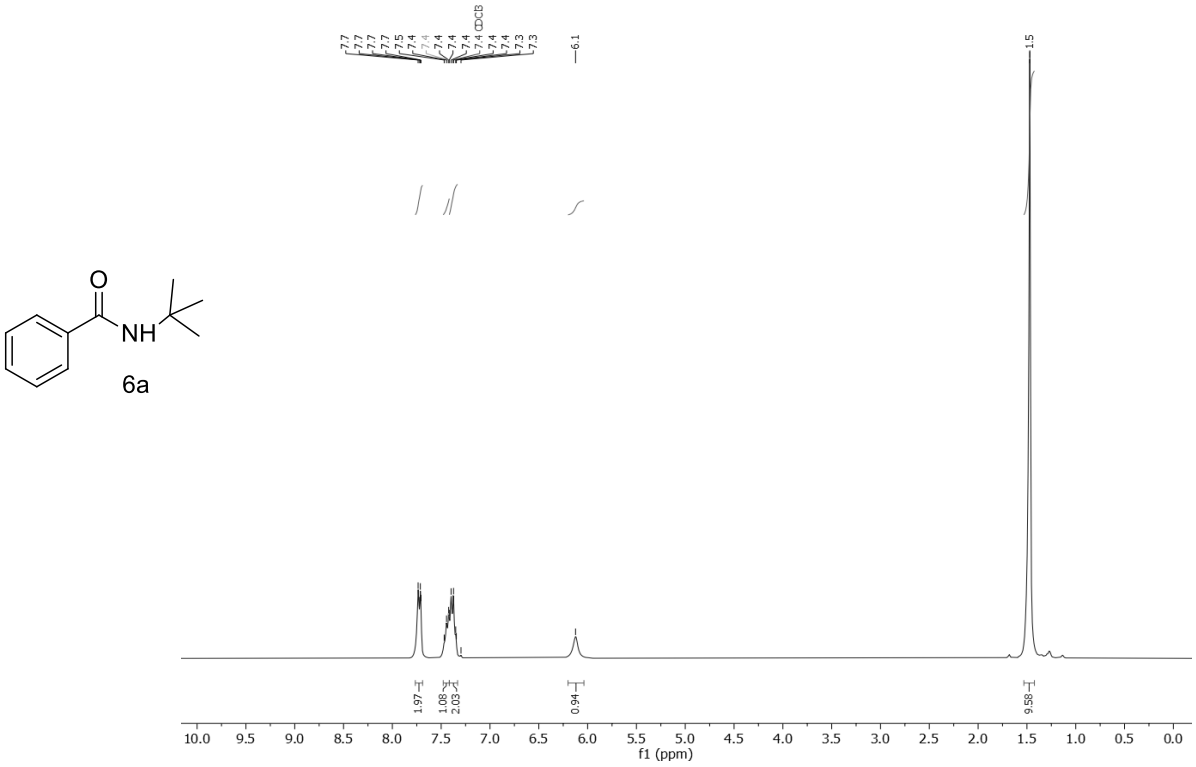
O
NH
6a
CDCl3
1.97
1.08
2.03
0.94
9.58
f1 (ppm)

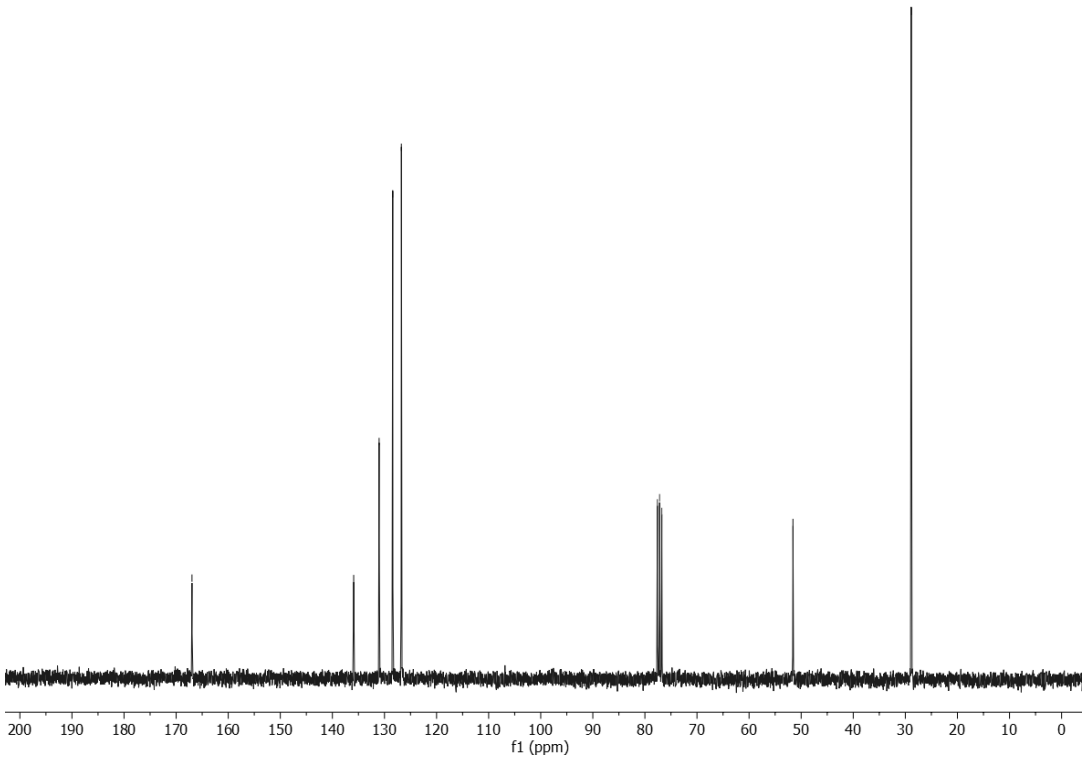
f1 (ppm)

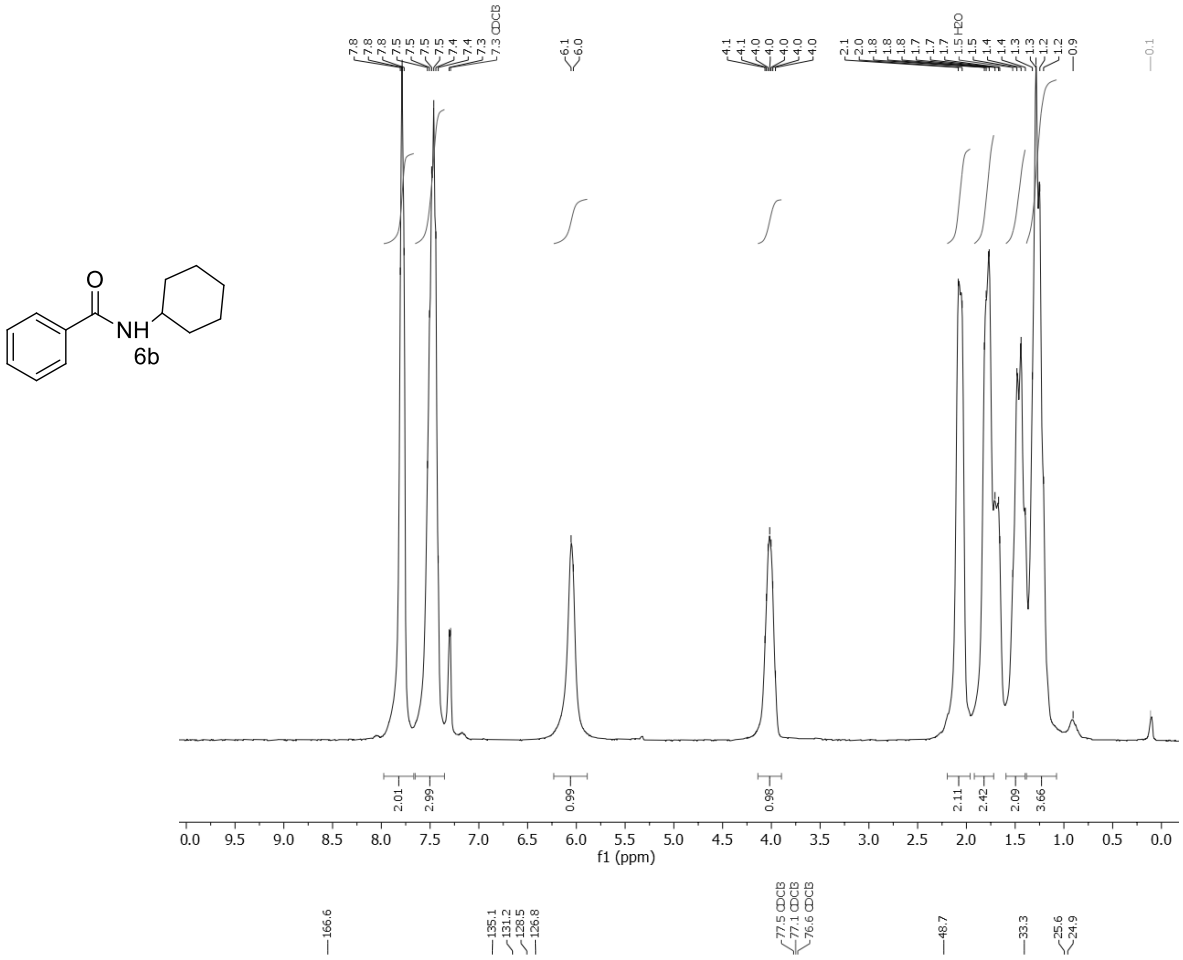
O
NH
6b
7.8
7.8
7.8
7.5
7.5
7.5
7.5
7.4
7.4
7.3
7.3 CDCl3
6.1
6.0
4.1
4.1
4.0
4.0
4.0
4.0
4.0
2.1
2.0
1.8
1.8
1.8
1.7
1.7
1.7
1.5 H2O
1.5
1.4
1.4
1.3
1.3
1.2
1.2
0.9
0.1
2.01
2.99
0.99
0.98
2.11
2.42
2.09
3.66
0.0 9.5 9.0 8.5 8.0 7.5 7.0 6.5 6.0 5.5 5.0 4.5 4.0 3.5 3.0 2.5 2.0 1.5 1.0 0.5 0.0
f1 (ppm)

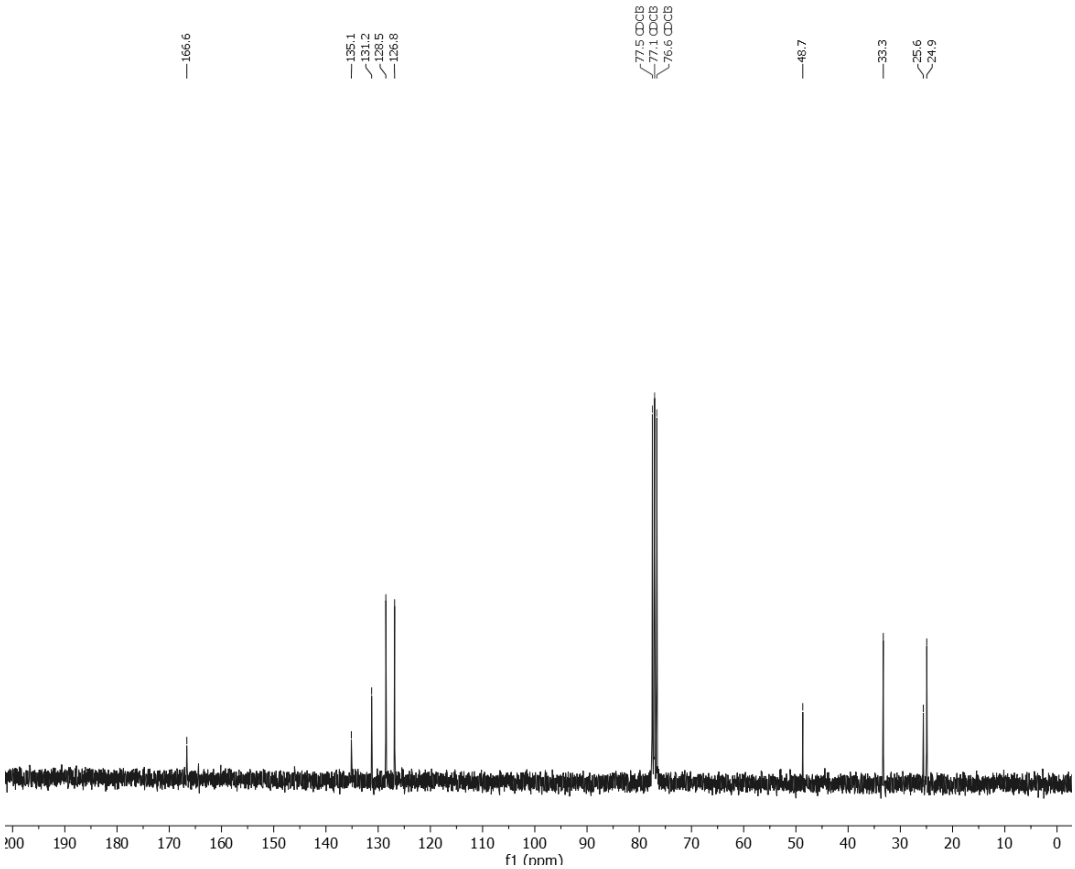
166.6
135.1
131.2
128.5
126.8
77.5 CDCl3
77.1 CDCl3
76.6 CDCl3
48.7
33.3
25.6
24.9
190 180 170 160 150 140 130 120 110 100 90 80 70 60 50 40 30 20 10 0
f1 (ppm)

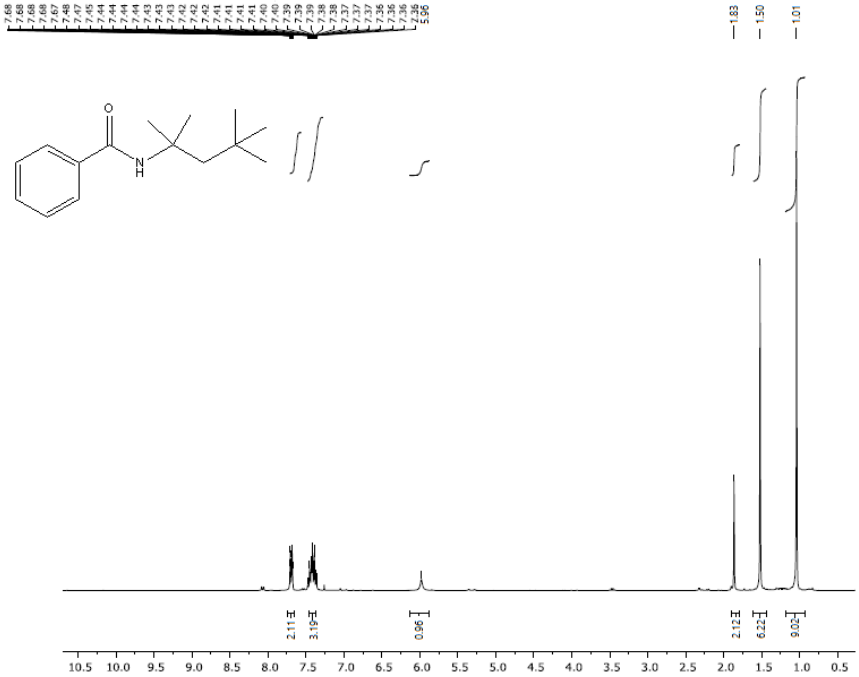
7.68
7.68
7.68
7.68
7.68
7.67
7.67
7.49
7.47
7.45
7.44
7.44
7.44
7.44
7.43
7.43
7.43
7.43
7.42
7.42
7.42
7.41
7.41
7.41
7.41
7.41
7.40
7.40
7.39
7.39
7.39
7.38
7.38
7.38
7.37
7.37
7.37
7.37
7.36
7.36
7.36
7.36
5.96
1.83
1.50
1.01
O
N
H
2.11
3.19
0.96
2.12
6.22
9.03
10.5 10.0 9.5 9.0 8.5 8.0 7.5 7.0 6.5 6.0 5.5 5.0 4.5 4.0 3.5 3.0 2.5 2.0 1.5 1.0 0.5

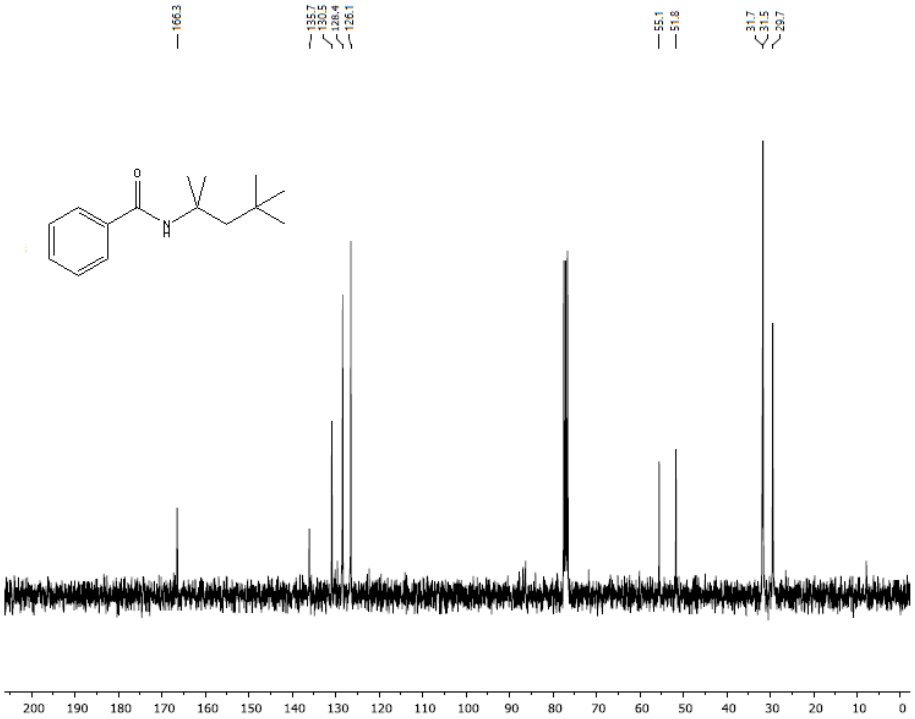
166.3
135.7
130.5
128.4
126.1
55.1
51.8
31.7
31.5
29.7
O
N
H
200 190 180 170 160 150 140 130 120 110 100 90 80 70 60 50 40 30 20 10 0

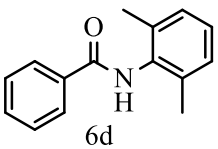

6d

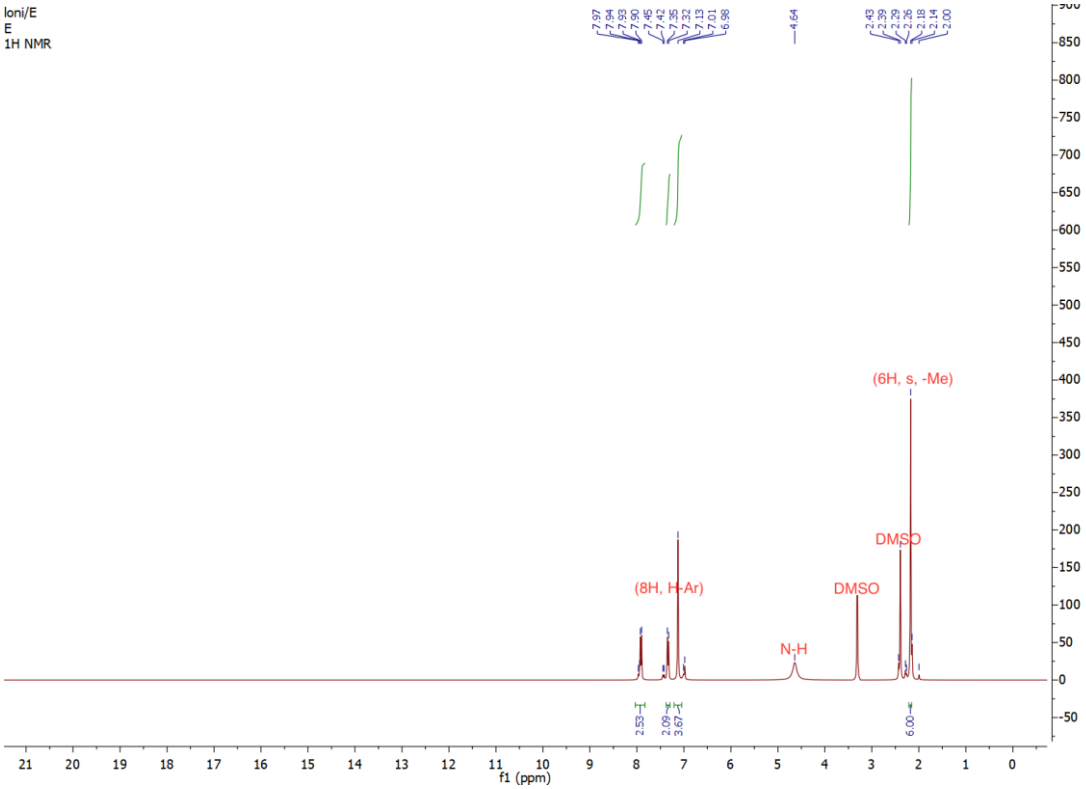
loni/E
E
1H NMR
(6H, s, -Me)
DMSO
DMSO
(8H, H-Ar)
N-H
f1 (ppm)

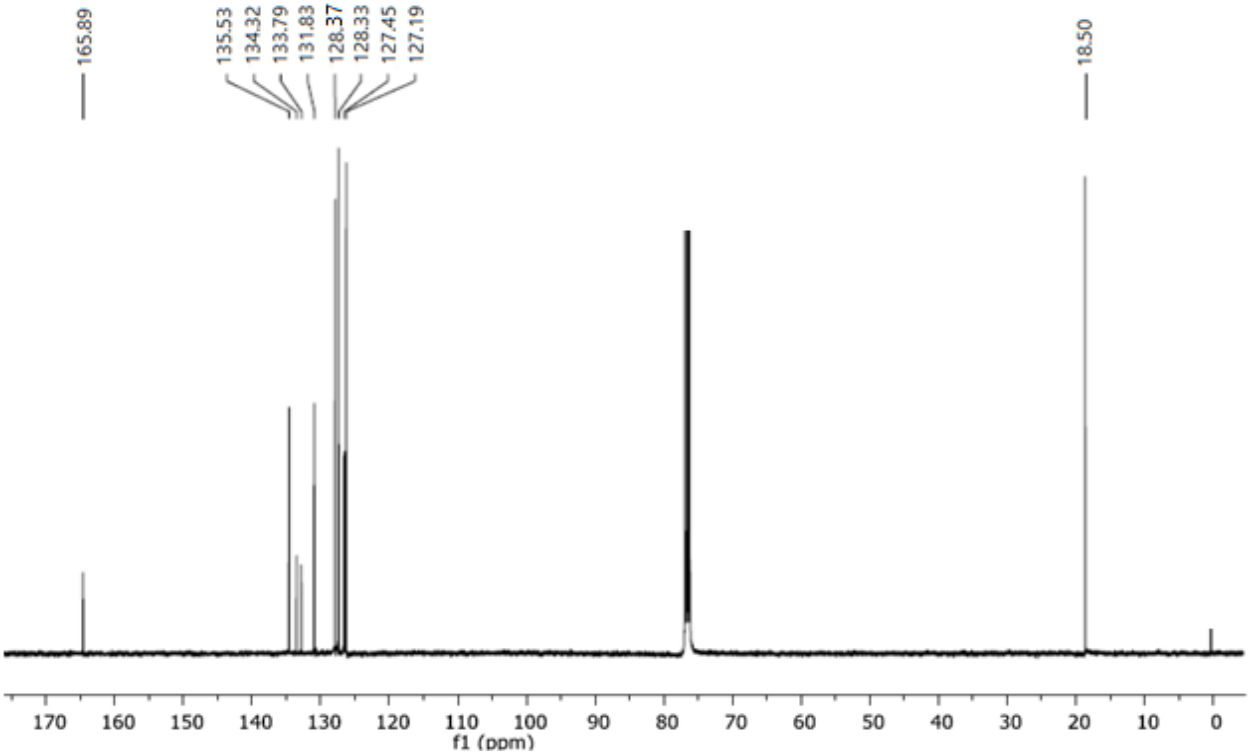
165.89
135.53
134.32
133.79
131.83
128.37
128.33
127.45
127.19
18.50
f1 (ppm)

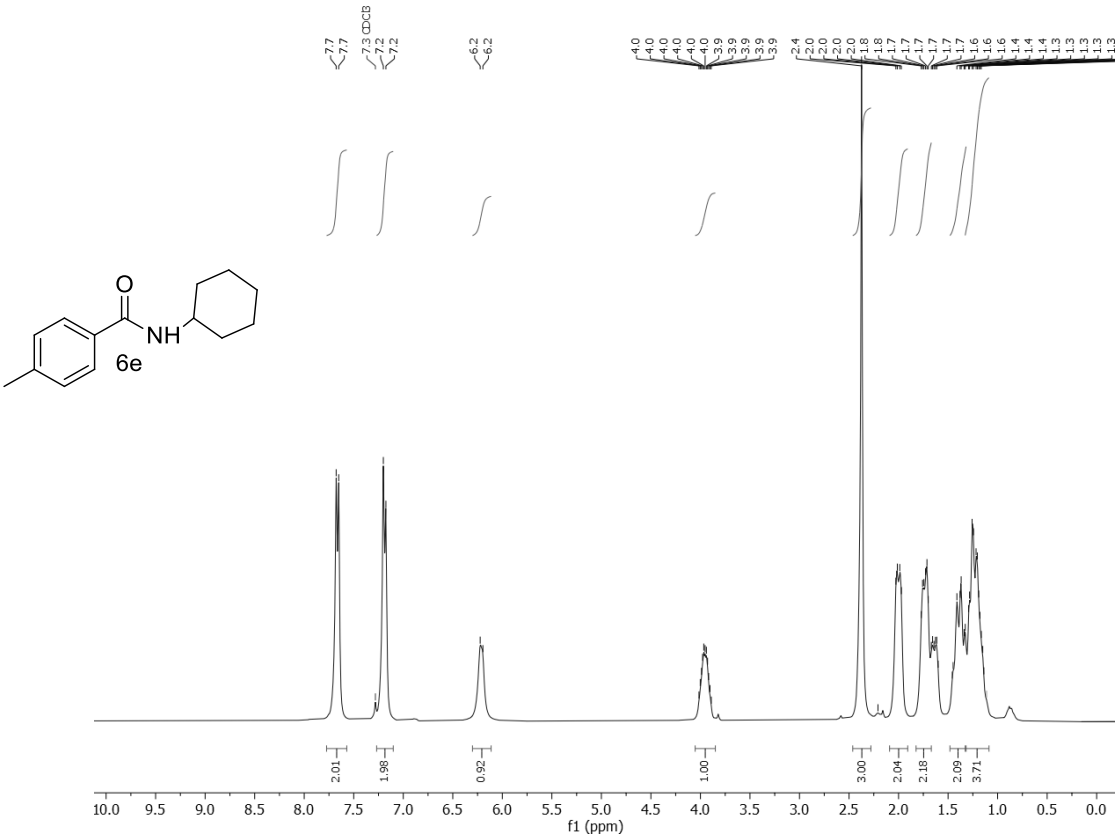
O
NH
6e
7.7
7.7
7.3 CDCl3
7.2
7.2
6.2
6.2
2.01
1.98
0.92
1.00
3.00
2.04
2.18
2.09
3.71
f1 (ppm)

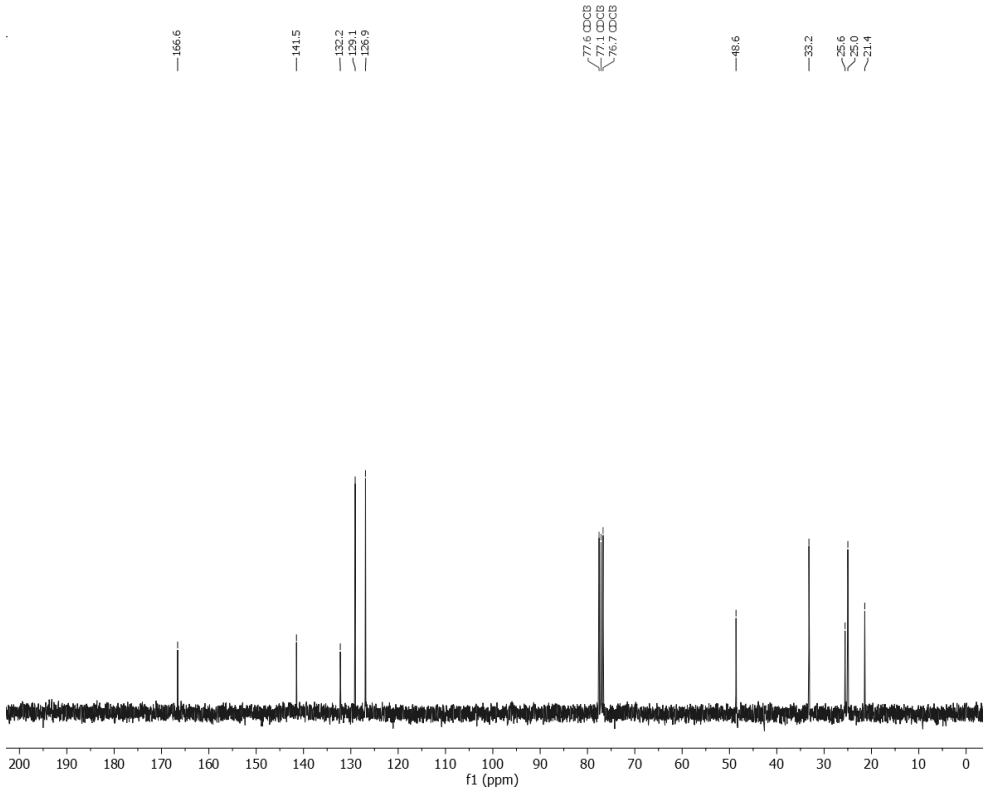
166.6
141.5
132.2
129.1
126.9
77.6 CDCl3
77.1 CDCl3
76.7 CDCl3
48.6
33.2
25.6
25.0
21.4
f1 (ppm)

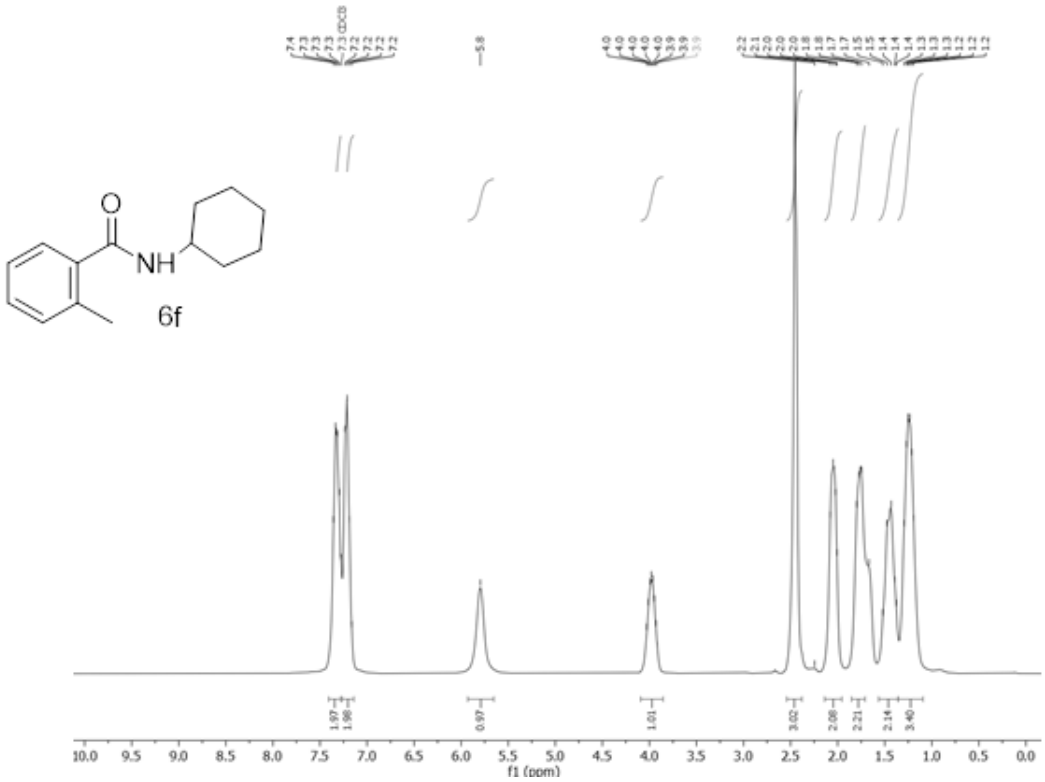
O
NH
6f
f1 (ppm)

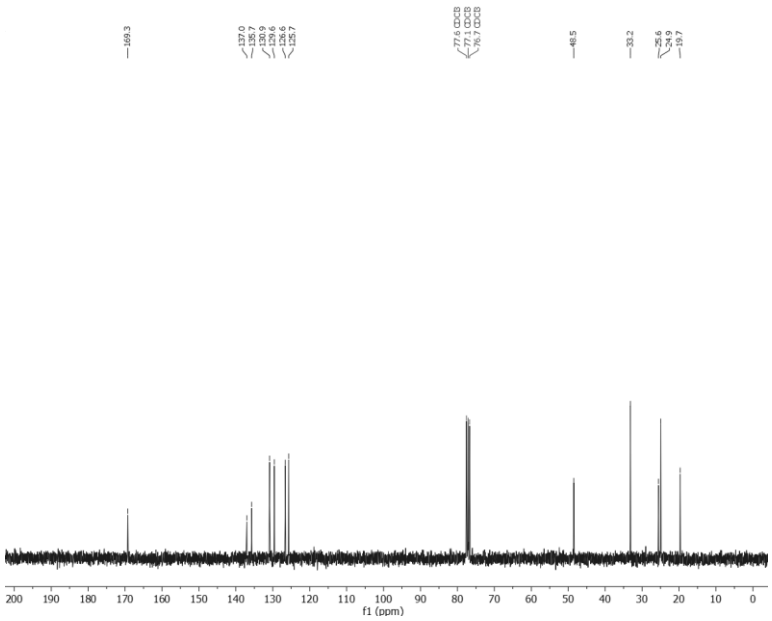
f1 (ppm)

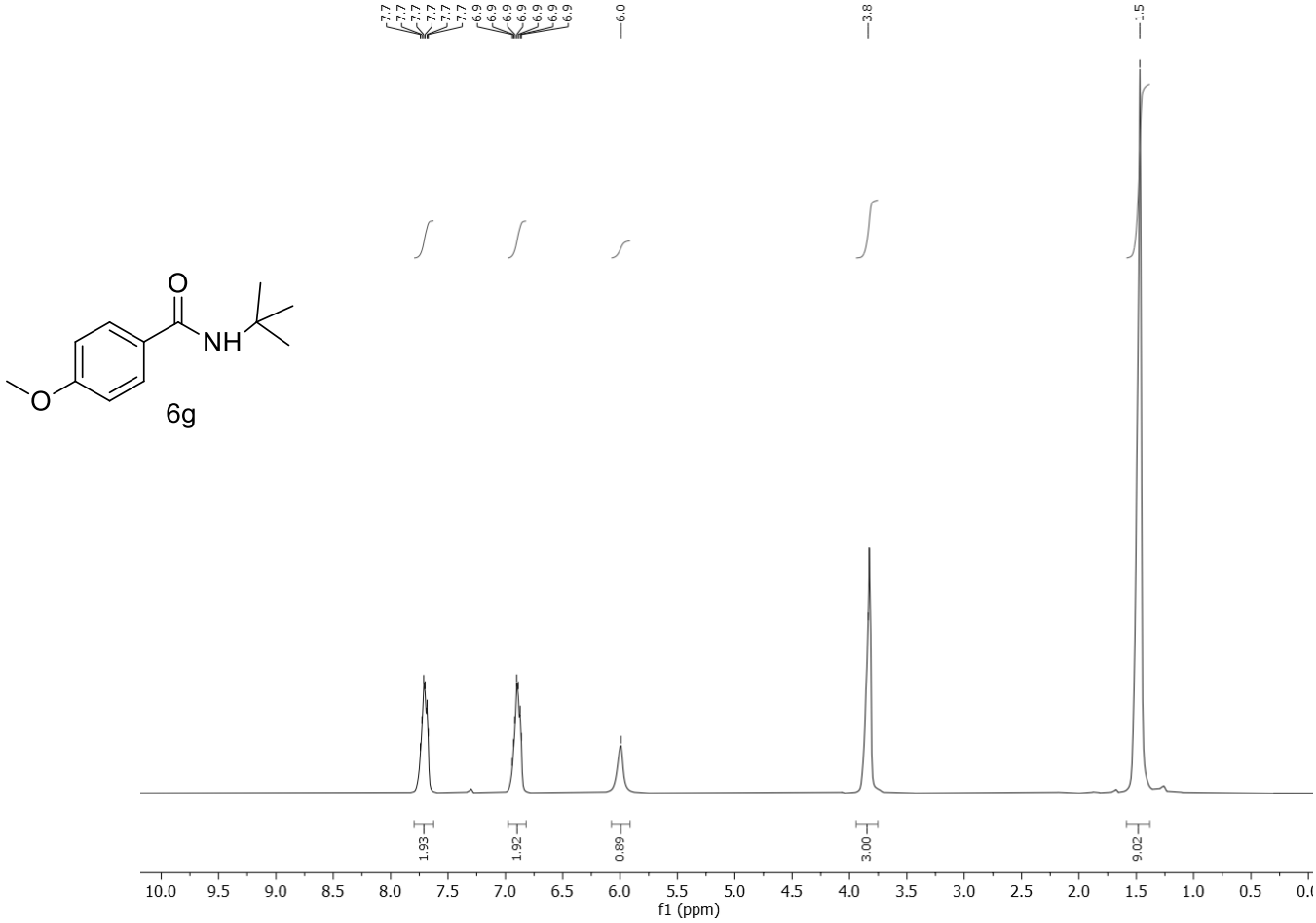
7.7
7.7
7.7
7.7
7.7
7.7
6.9
6.9
6.9
6.9
6.9
6.9
6.9
6.0
3.8
1.5
O
NH
O
6g
1.93
1.92
0.89
3.00
9.02
10.0 9.5 9.0 8.5 8.0 7.5 7.0 6.5 6.0 5.5 5.0 4.5 4.0 3.5 3.0 2.5 2.0 1.5 1.0 0.5
f1 (ppm)

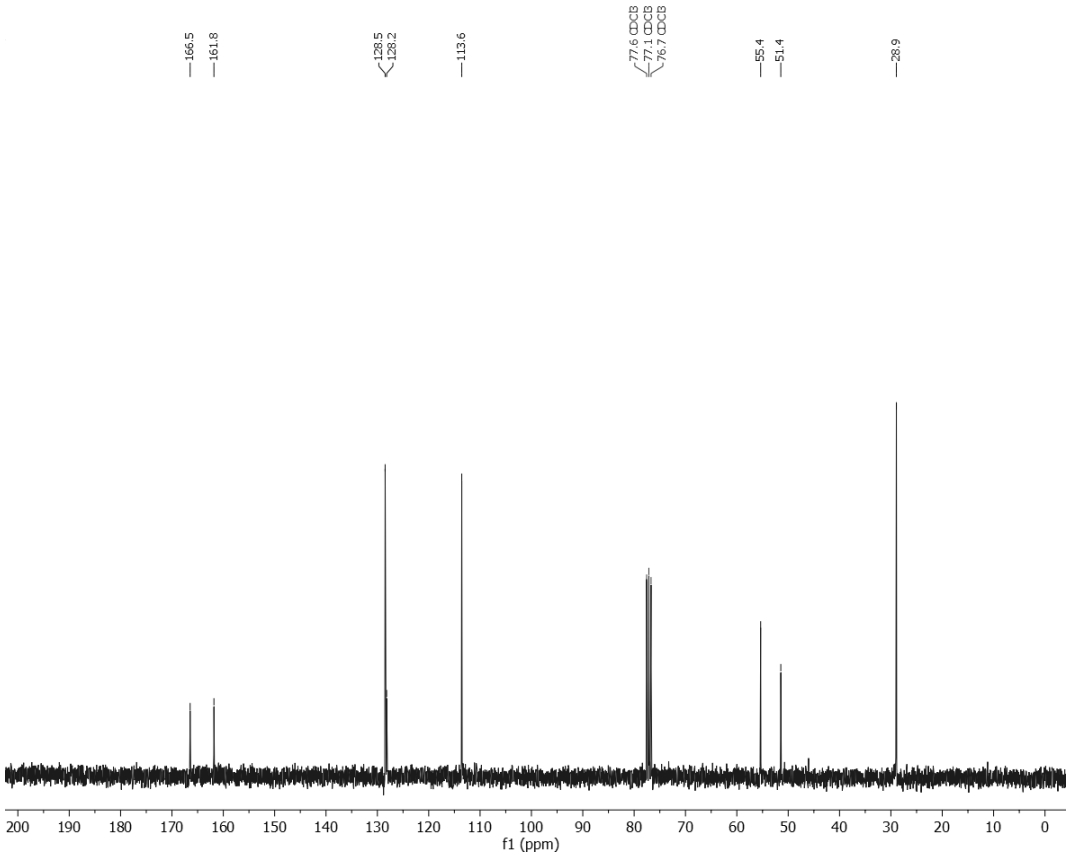
166.5
161.8
128.5
128.2
113.6
77.6 CDCl3
77.1 CDCl3
76.7 CDCl3
55.4
51.4
28.9
200 190 180 170 160 150 140 130 120 110 100 90 80 70 60 50 40 30 20 10 0
f1 (ppm)

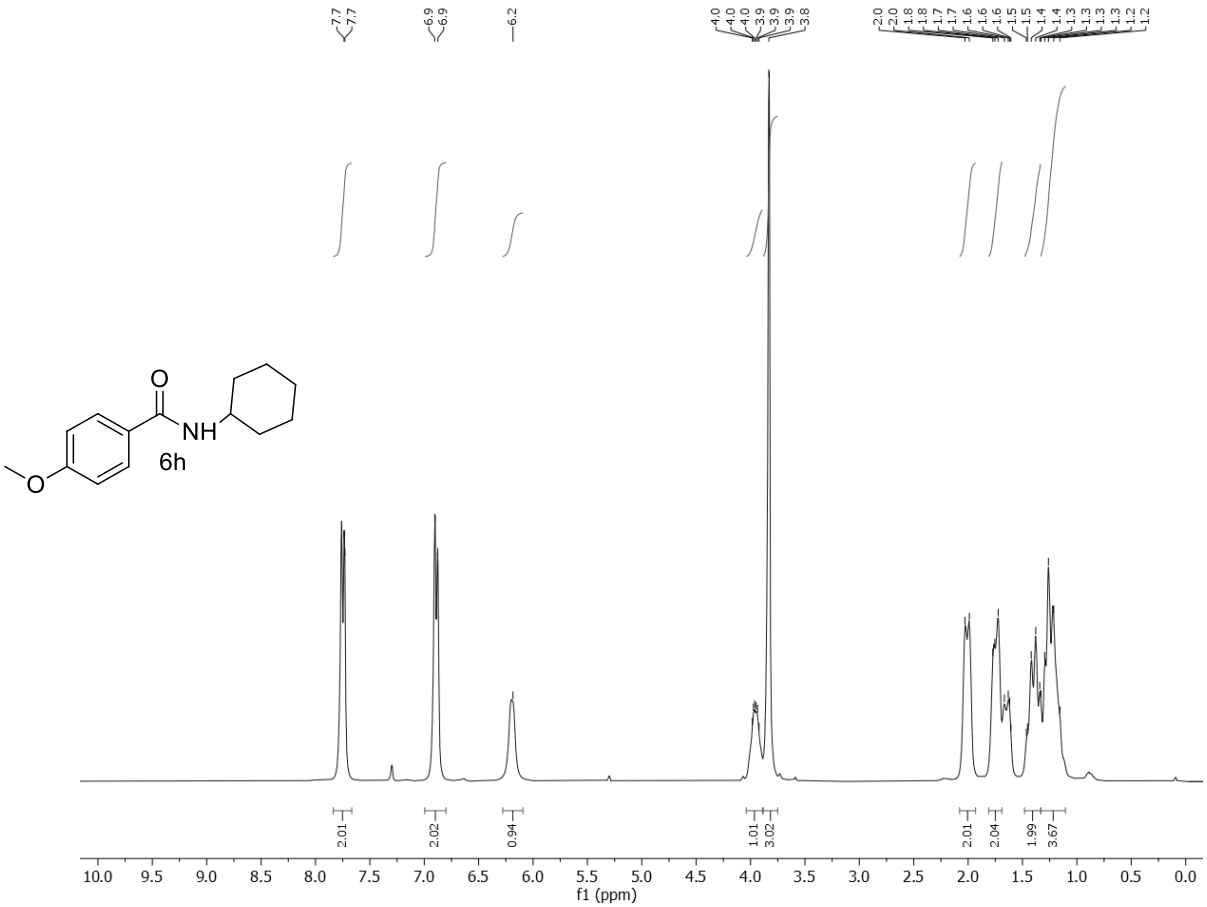
6h
f1 (ppm)

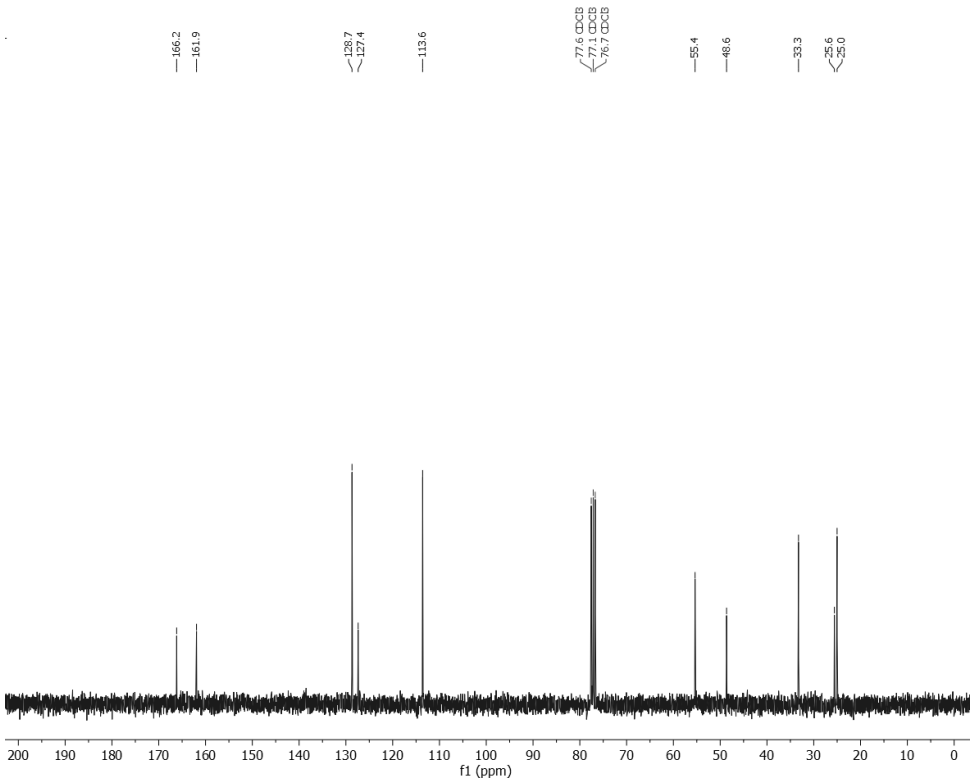
f1 (ppm)

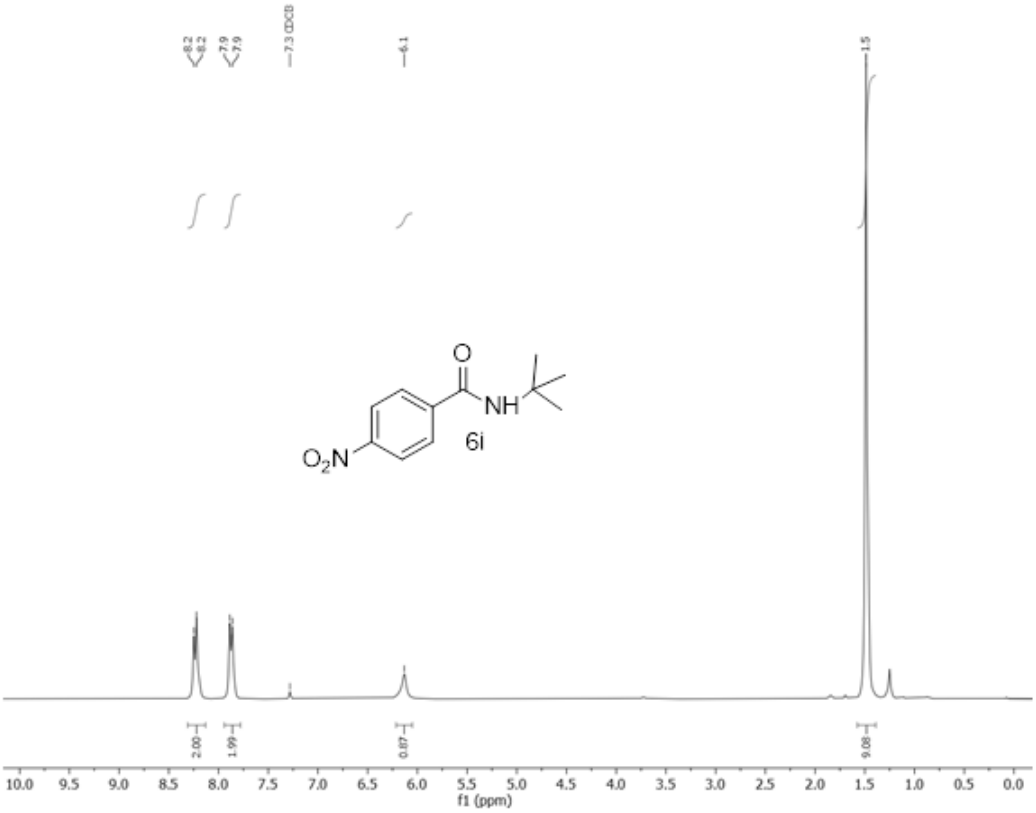
8.2
8.2
7.9
7.9
7.3 CDCl3
6.1
1.5
O
NH
O_2N
6i
2.00
1.99
0.87
9.08
10.0 9.5 9.0 8.5 8.0 7.5 7.0 6.5 6.0 5.5 5.0 4.5 4.0 3.5 3.0 2.5 2.0 1.5 1.0 0.5 0.0
f1 (ppm)

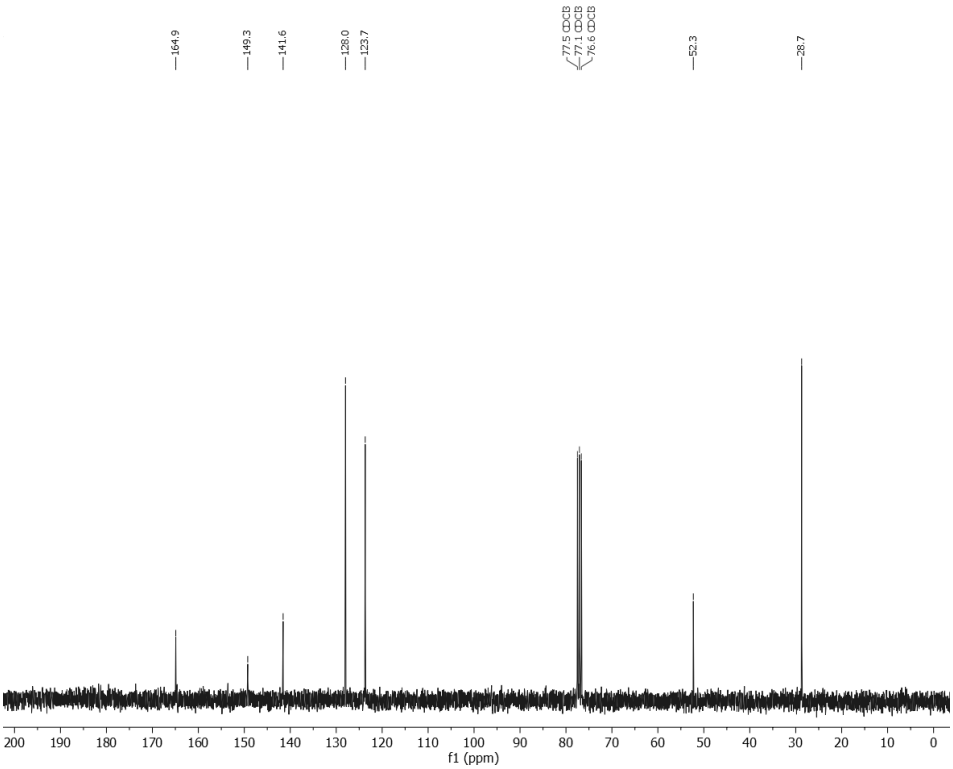
164.9
149.3
141.6
128.0
123.7
77.5 CDCl3
77.1 CDCl3
76.6 CDCl3
52.3
28.7
200 190 180 170 160 150 140 130 120 110 100 90 80 70 60 50 40 30 20 10 0
f1 (ppm)

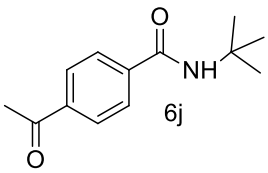
O
NH
O

6j

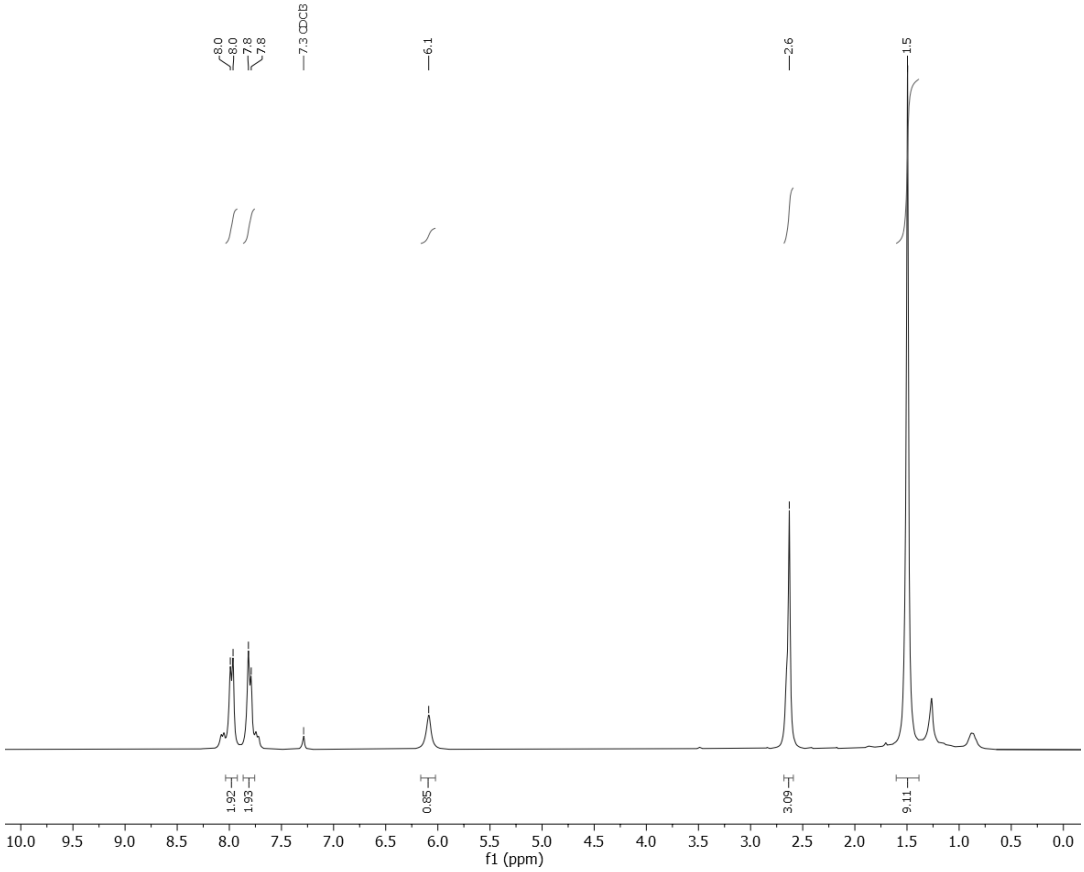
8.0
8.0
7.8
7.8
7.3 CDCl3
6.1
2.6
1.5
1.92
1.93
0.85
3.09
9.11
10.0 9.5 9.0 8.5 8.0 7.5 7.0 6.5 6.0 5.5 5.0 4.5 4.0 3.5 3.0 2.5 2.0 1.5 1.0 0.5 0.0
f1 (ppm)

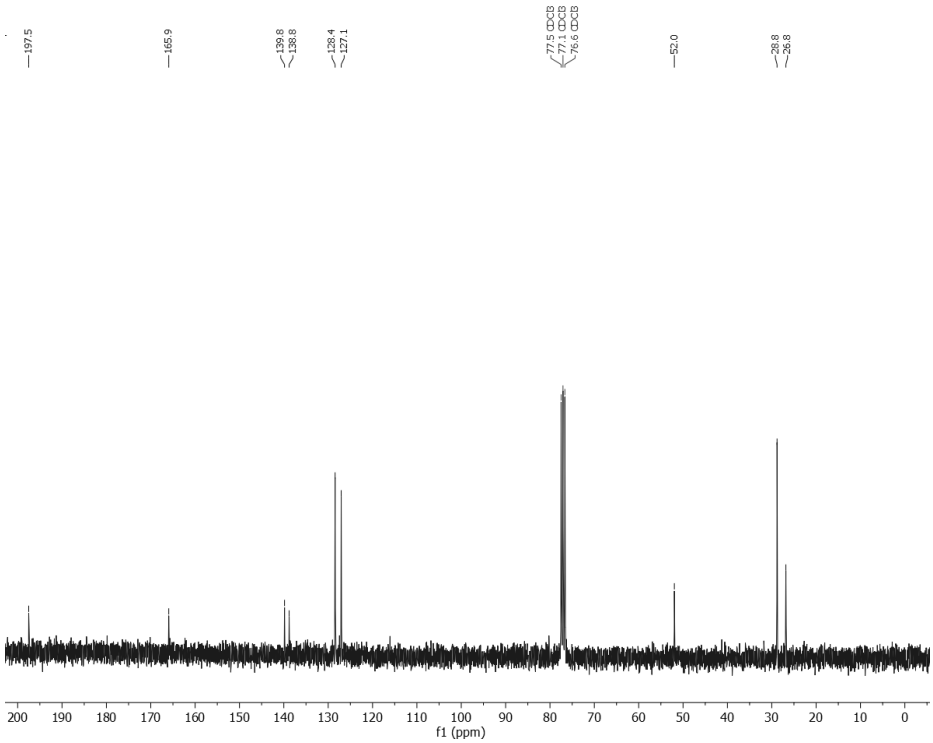
197.5
165.9
139.8
138.8
128.4
127.1
77.5 CDCl3
77.1 CDCl3
76.6 CDCl3
52.0
28.8
26.8
200 190 180 170 160 150 140 130 120 110 100 90 80 70 60 50 40 30 20 10 0
f1 (ppm)

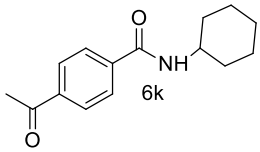
O
NH
O

6k

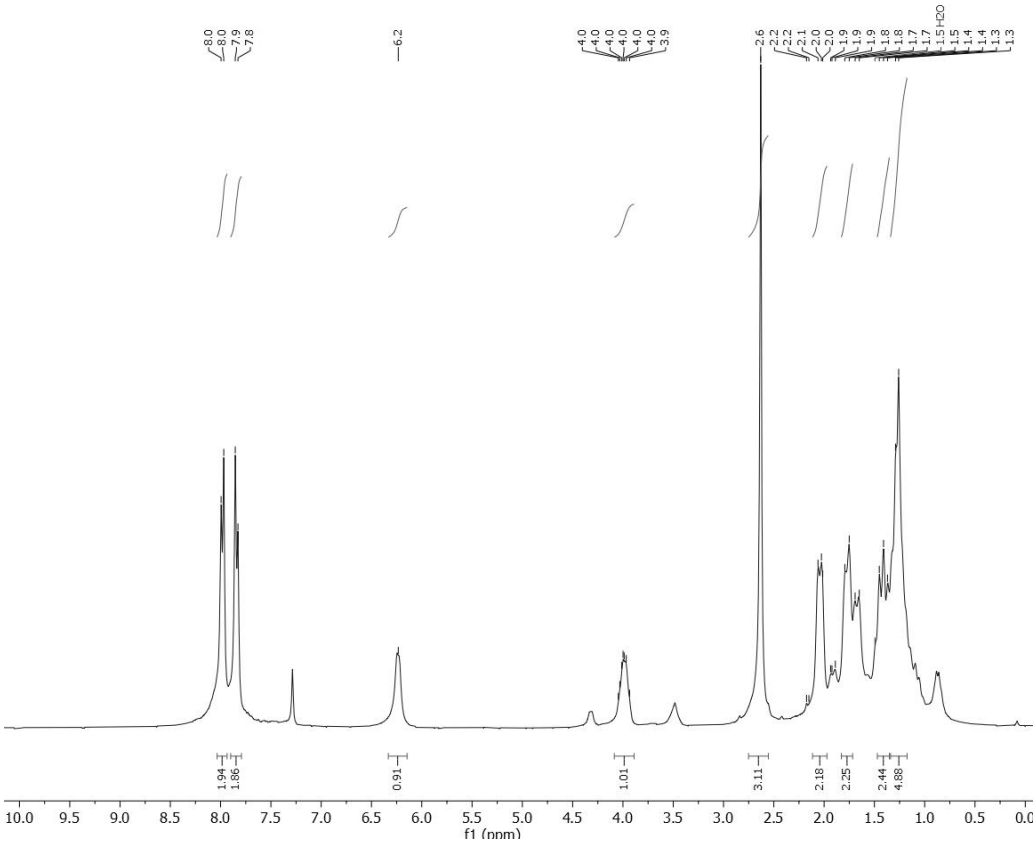
8.0
8.0
7.9
7.8
6.2
4.0
4.0
4.0
4.0
4.0
4.0
3.9
2.6
2.2
2.2
2.1
2.0
2.0
1.9
1.9
1.9
1.8
1.8
1.7
1.7
1.5 H2O
1.5
1.4
1.4
1.3
1.3
1.94
1.86
0.91
1.01
3.11
2.18
2.25
2.44
4.88
10.0 9.5 9.0 8.5 8.0 7.5 7.0 6.5 6.0 5.5 5.0 4.5 4.0 3.5 3.0 2.5 2.0 1.5 1.0 0.5 0.0
f1 (ppm)

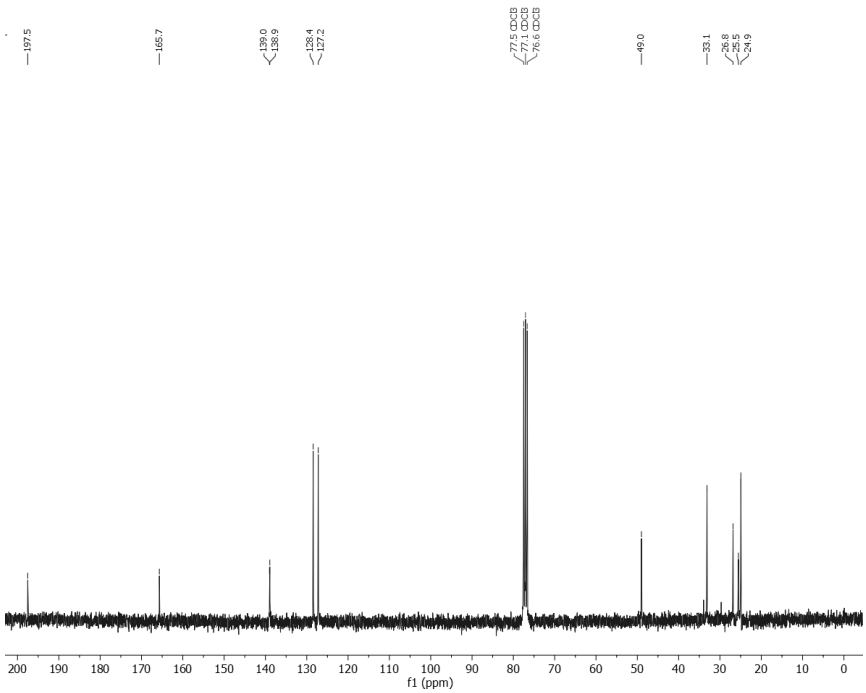
197.5
165.7
139.0
138.9
128.4
127.2
77.5 CDCl3
77.1 CDCl3
76.6 CDCl3
49.0
33.1
26.8
25.5
24.9
200 190 180 170 160 150 140 130 120 110 100 90 80 70 60 50 40 30 20 10 0
f1 (ppm)

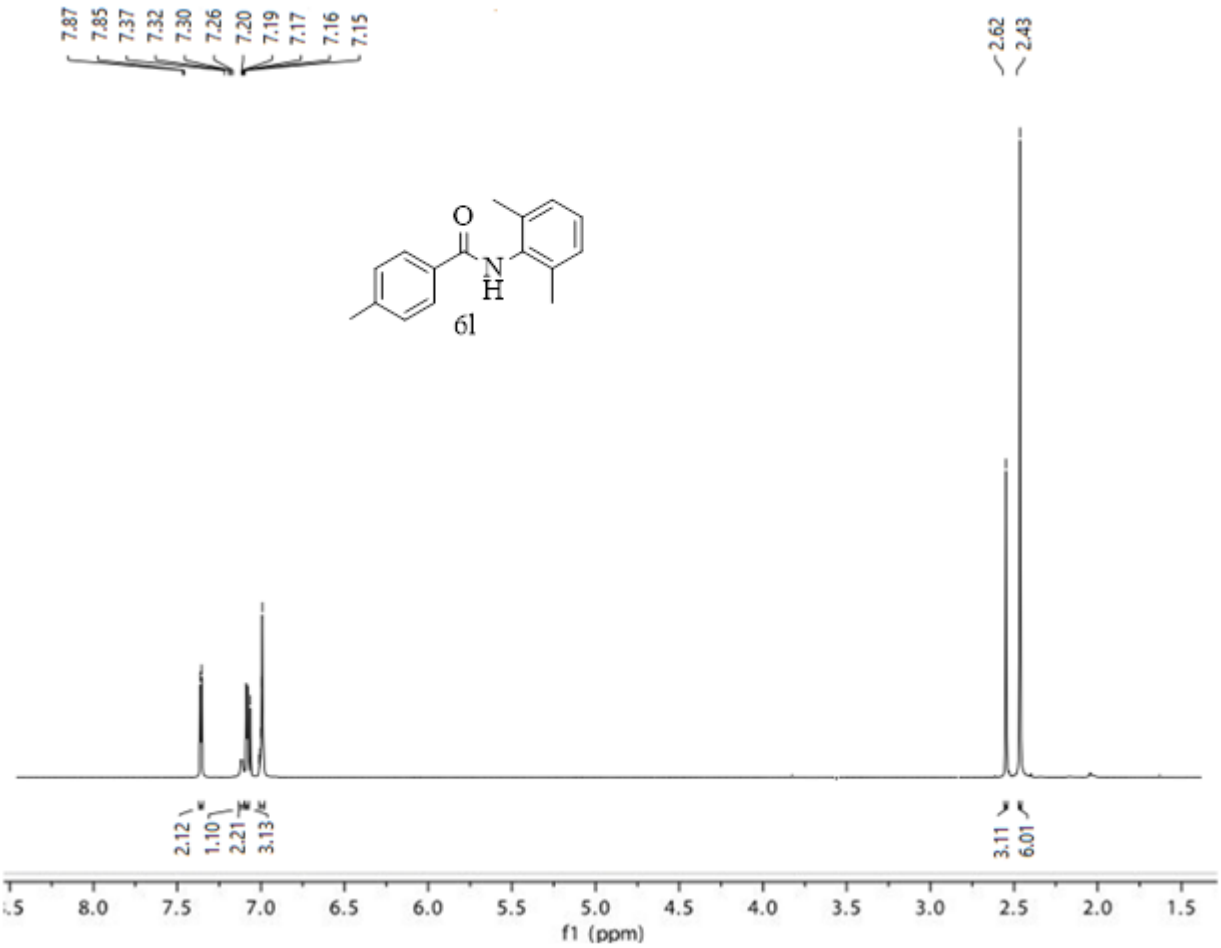
7.87
7.85
7.37
7.32
7.30
7.26
7.20
7.19
7.17
7.16
7.15
2.62
2.43
O
N
H
6l
2.12
1.10
2.21
3.13
3.11
6.01
8.0
7.5
7.0
6.5
6.0
5.5
5.0
4.5
4.0
3.5
3.0
2.5
2.0
1.5
f1 (ppm)

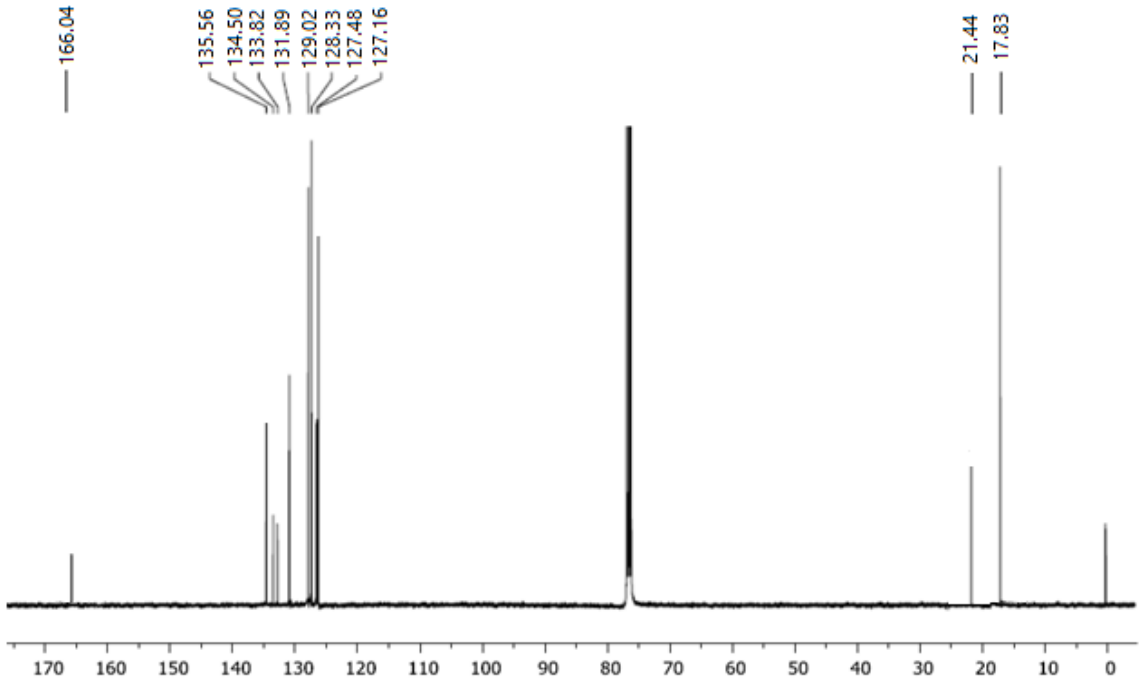
166.04
135.56
134.50
133.82
131.89
129.02
128.33
127.48
127.16
21.44
17.83
170
160
150
140
130
120
110
100
90
80
70
60
50
40
30
20
10
0

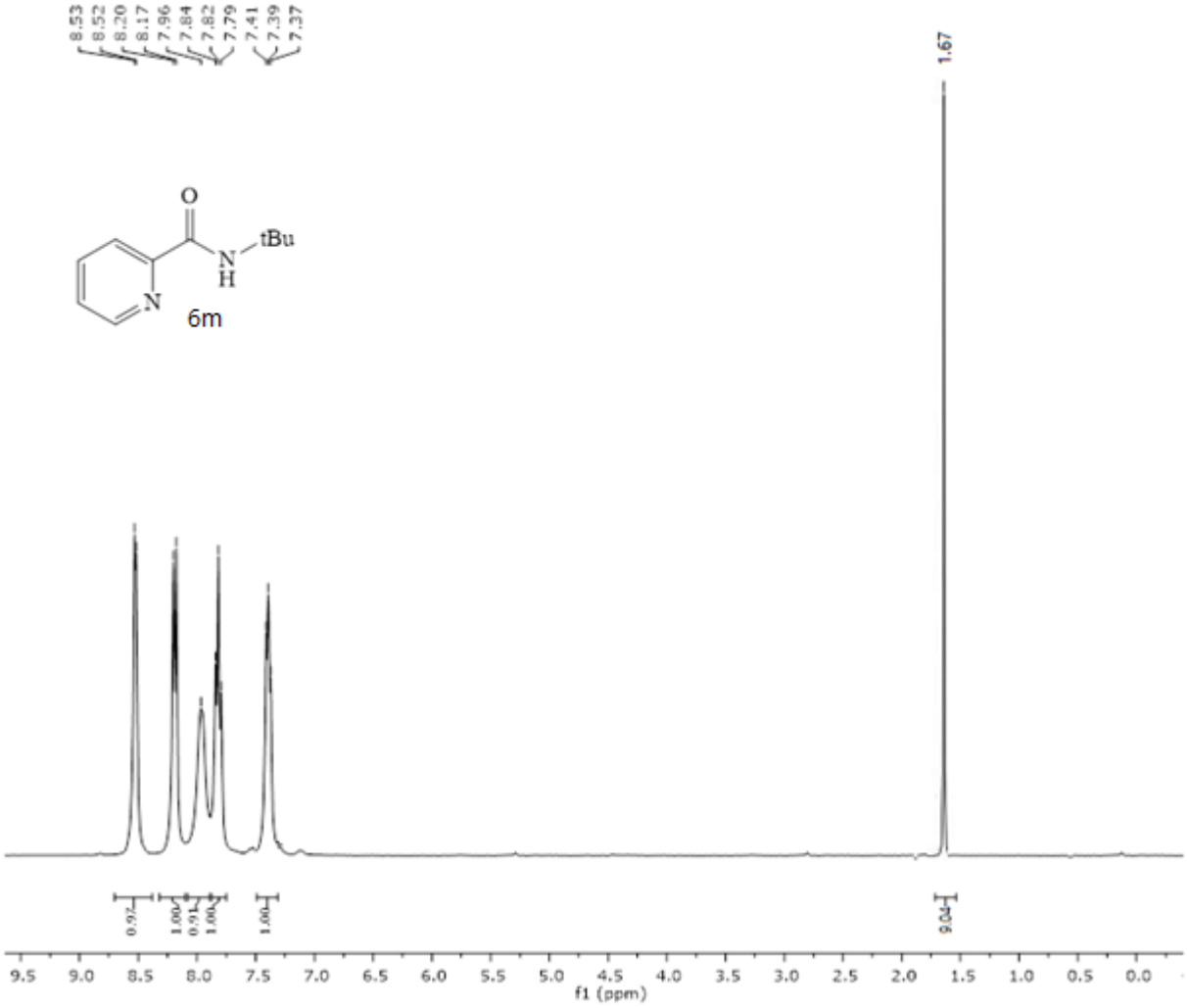
8.53
8.52
8.20
8.17
7.96
7.84
7.82
7.79
7.41
7.39
7.37
1.67
O
tBu
N
H
N
6m
0.97
1.00
0.91
1.00
1.00
9.04
9.5 9.0 8.5 8.0 7.5 7.0 6.5 6.0 5.5 5.0 4.5 4.0 3.5 3.0 2.5 2.0 1.5 1.0 0.5 0.0
f1 (ppm)

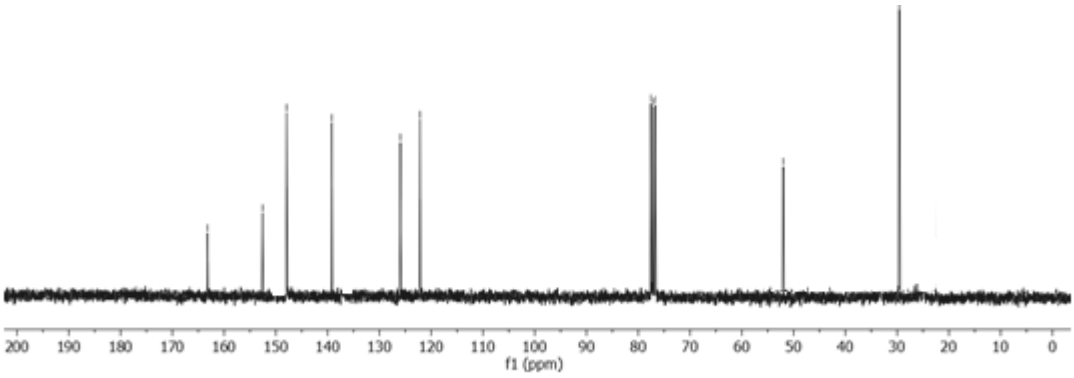
200 190 180 170 160 150 140 130 120 110 100 90 80 70 60 50 40 30 20 10 0
f1 (ppm)

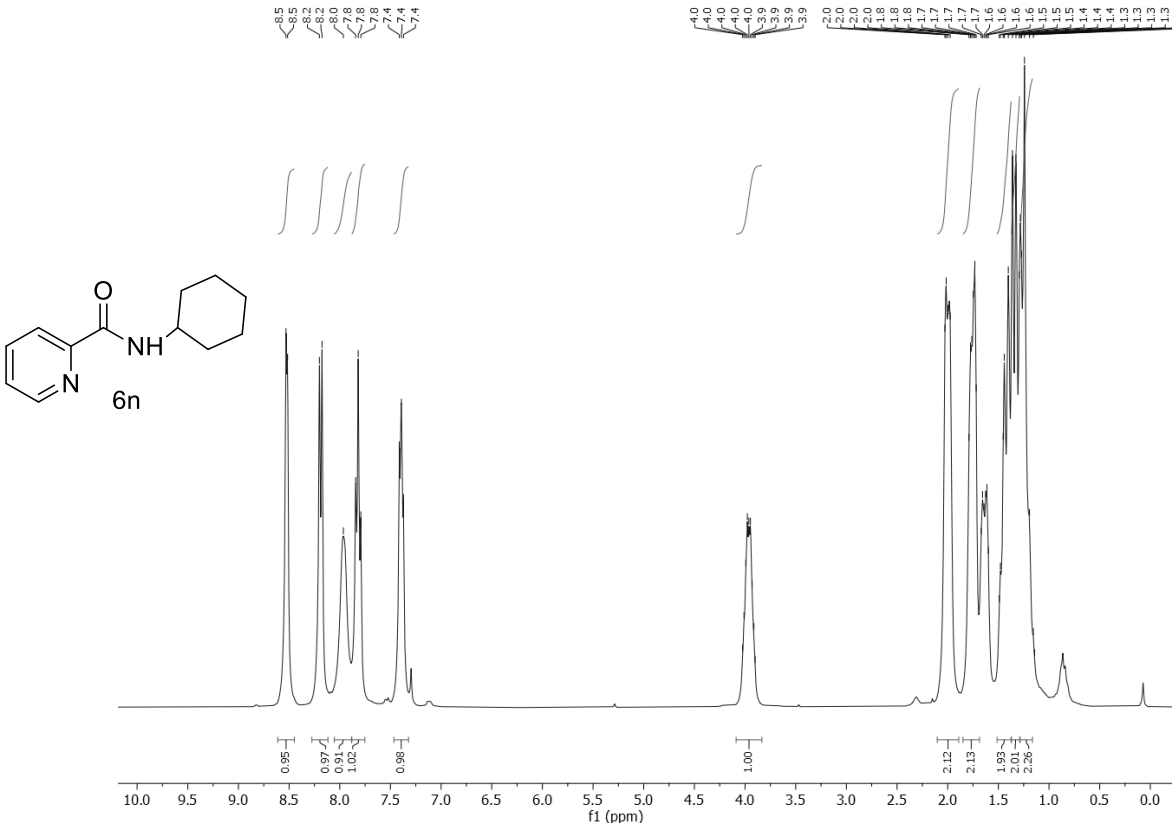
O
NH
N
6n
f1 (ppm)

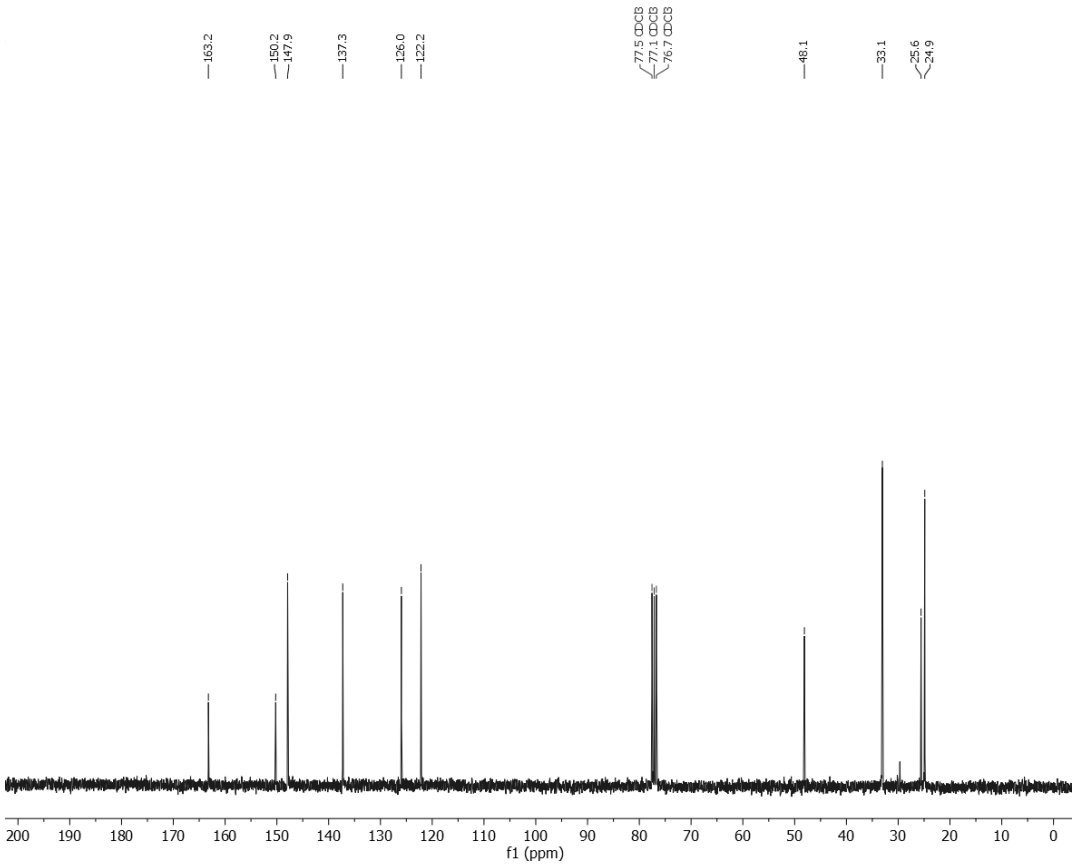
163.2
150.2
147.9
137.3
126.0
122.2
77.5 CDCl3
77.1 CDCl3
76.7 CDCl3
48.1
33.1
25.6
24.9
f1 (ppm)